AD-A155 974

②

APERTURE ANTENNA EFFECTS AFTER PROPAGATION THROUGH STRONGLY DISTURBED RANDOM MEDIA

Dennis L. Knepp
Mission Research Corporation
P.O. Drawer 719
Santa Barbara, CA 93102-0719

1 February 1984

Technical Report

Prepared for
    Director
    DEFENSE NUCLEAR AGENCY
    Washington, DC 20305-1000

DTIC
ELECTE
JUL 1 1985

B

20000814028

85   5   03   034

REPORT DOCUMENTATION PAGE		READ INSTRUCTIONS BEFORE COMPLETING FORM
1. REPORT NUMBER DNA-TR-84-80	2. GOVT ACCESSION NO. AD-A155974	3. RECIPIENT'S CATALOG NUMBER
4. TITLE (and Subtitle) APERTURE ANTENNA EFFECTS AFTER PROPAGATION THROUGH STRONGLY DISTURBED RANDOM MEDIA		5. TYPE OF REPORT & PERIOD COVERED Technical Report
		6. PERFORMING ORG. REPORT NUMBER MRC-R-819
7. AUTHOR(s) Dennis L. Knepp		8. CONTRACT OR GRANT NUMBER(s) DNA 001-81-C-0006
9. PERFORMING ORGANIZATION NAME AND ADDRESS Mission Research Corporation PO Drawer 719 Santa Barbara, California 93102-0719		10. PROGRAM ELEMENT, PROJECT, TASK AREA & WORK UNIT NUMBERS DNA 001-83-C-0021
11. CONTROLLING OFFICE NAME AND ADDRESS Director Defense Nuclear Agency Washington, DC 20305-1000		12. REPORT DATE 1 February 1984
		13. NUMBER OF PAGES 64
14. MONITORING AGENCY NAME & ADDRESS(if different from Controlling Office)		15. SECURITY CLASS (of this report) UNCLASSIFIED
		15a. DECLASSIFICATION DOWNGRADING SCHEDULE N/A since UNCLASSIFIED

16. DISTRIBUTION STATEMENT (of this Report)

Approved for public release; distribution is unlimited.

17. DISTRIBUTION STATEMENT (of the abstract entered in Block 20, if different from Report)

19. KEY WORDS (Continue on reverse side if necessary and identify by block number)

Aperture Antennas	Random Media
Space Based Radar	Dispersive Media
Signal Scintillation	Satellite Communications
Ionospheric Propagation	Frequency Selective Environment

20. ABSTRACT (Continue on reverse side if necessary and identify by block number)

A strongly disturbed layer of ionization irregularities that is used as a propagation channel for radio waves can degrade the propagating wave and thereby affect the resulting measurements at the receiving antenna. The antenna aperture itself also affects measurements of the received signal by its inherent averaging process. Here an analytic solution for the two-position, two-frequency mutual coherence function, valid in the strong-scatter limit, is used to characterize the propagation

DD FORM 1473 1 JAN 73   EDITION OF 1 NOV 65 IS OBSOLETE

20. Abstract (Continued)

channel. The channel itself consists of a thick slab of anisotropic elec-
tron density irregularities that are elongated in the direction parallel
to the earth's magnetic field.

Analytic expressions are obtained that give the effect of the
aperture antenna on measurements of received power, decorrelation time (or
distance), mean time delay, time delay jitter and coherence bandwidth.
These quantities are determined as functions of the aperture diameter and
of the angle between the magnetic field and the direction of propagation.
It is shown that in strong turbulence aperture averaging can be a signi-
ficant factor in reducing the received power by angular scattering loss,
increasing the observed signal decorrelation time via aperture averaging,
and reducing the time delay jitter by suppression of signals received at
off-boresight angles.

Results are presented for two cases. One-way propagation
through an ionospheric communication channel is considered where both
transmitter and receiver utilize aperture antennas. This result is easily
extended to the case that one of the antennas is an omnidirectional point
source, corresponding to the usual case of transionospheric satellite
communication from a small satellite antenna to a large ground based
receiver. The second case involves transmission and reception of a radar
signal that travels through a disturbed ionospheric channel to a target
located in free space. This case is applicable to the situation of a
large antenna aboard a space based radar or to the case of a ground based
defense radar.

SUMMARY

In this report analytic expressions are derived for the effect of aperture antennas on measurements of signals that have propagated through strong anisotropic turbulence. Results are given for the effect of Gaussian apertures on measurements of received signal power, decorrelation distance (or time), mean time delay and time delay jitter. The geometries considered correspond to the case of a single, one-way propagation path between two aperture antennas located in free space and separated by a layer of turbulence and to the case of a monostatic radar where radar and target are on opposite sides of a strong scattering layer.

All calculations depend on the analytic solution for the two-position, two-frequency mutual coherence function for spherical wave propagation in an anisotropic layer of electron density irregularities. The analytic solution for propagation in a thick layer is derived here using the quadratic phase structure-function approximation valid for strong turbulence. This result is then specialized to a thin phase-screen approximation to facilitate analytic calculation of the effects of apertures.

It is shown that antennas that are larger in diameter than the decorrelation distance that would be measured by an omnidirectional antenna can experience significant angular scattering loss and exhibit increased measurements of decorrelation distance, and decreased measurements of mean time delay and time delay jitter. Increased measurements of signal decorrelation distance are caused by the averaging effect of the antenna aperture that smooths (eliminates) the small scale signal fluctua-

1

tions. Decreased measurements of mean time delay and time delay jitter are caused by the action of the aperture to cut off signal contributions that originate from off-boresight angles and have therefore exper'enced more time delay than experienced over more direct signal paths.

Generally, the effects of aperture averaging first begin to be significant for aperture sizes that approach ten times the decorrelation distance measured with a point antenna. For even larger apertures, the aperture has a significant effect on the received signal at the antenna output that can be computed using the formulas and curves provided herein.

PREFACE

DTIC
COPY
INSPECTED
1

Accession For	
NTIS GRA&I	☑
DTIC TAB	☐
Unannounced	☐
Justification	
By	
Distribution/	
Availability Codes	
Dist	Avail and/or Special
A-1	

TABLE OF CONTENTS

LIST OF ILLUSTRATIONS

LIST OF·ILLUSTRATIONS (Concluded)

SECTION 1
INTRODUCTION

Large high-gain antennas are used in many radar and communications applications to increase the energy collected, to increase angular accuracy, and to provide protection against jamming. If the wavefront at the antenna aperture experiences scintillation, large apertures can act to average the signal and thereby modify the observed signal properties. In the late fifties Wheelon (1957, 1959) obtained the well-known aperture smoothing effect for the measurement of phase fluctuations by a finite circular aperture. Since then, various investigators have studied the aperture smoothing effect on intensity scintillations in the optics regime (Fried, 1967; Tatarskii, 1971; Homstad et al., 1974) and also the related effect of optical beam wave propagation to an infinitesimal receiver (Lee and Harp, 1969; Ishimaru, 1969). Knepp (1975) obtained results for the effects of an antenna aperture on measurements of the in-phase and quadrature components and their spatial derivatives, for the case of weak scattering.

Scintillation or rapid variations in the amplitude, phase, and angle-of-arrival of a propagating wave is often observed over satellite links at VHF and UHF. Scintillation can also be observed at frequencies as high as the GHz range (Pope and Fritz, 1971; Skinner et al., 1971; Taur, 1976) and is occasionally severe, even at L-band (Fremouw et al., 1978). However, aperture averaging is not generally important at satellite frequencies (UHF-GHz) under ambient or naturally perturbed ionospheric conditions.

Worst case or Rayleigh amplitude scintillation is likely to occur if the ionosphere is highly disturbed, as for example by high altitude nuclear explosions (Arendt and Soicher, 1964; King and Fleming, 1980) or by chemical releases (Davis et al., 1974; Wolcott et al., 1978). Increased electron concentrations and the irregular structure of the ionization can lead to intense Rayleigh signal scintillation at frequencies as high as the 7-8 GHz SHF band (Knepp, 1977). Consequently, the effects of scintillation are important to any UHF through SHF communications or radar system that must operate through an ionospheric channel and that may have to operate in highly disturbed propagation environments.

For cases of severe scintillation where the signal varies across the area of the receiving aperture, the effect of the aperture can be significant. It is well known that an aperture antenna acts to cut off energy that is incident at off-boresight angles where the antenna gain is reduced. This effect may also be viewed as the result of averaging or coherent processing of the electromagnetic field intercepted at the aperture location. In this report the effects of aperture averaging are analytically calculated for the case where Gaussian antenna beams are used by transmitter and receiver. Results are presented for two different physical situations. One-way propagation through an ionospheric communication channel is considered where both transmitter and receiver utilize aperture antennas. This result is easily extended to the case that one of the antennas is a point source, corresponding to the usual case of trans-ionospheric satellite communications. The second antenna geometry corresponds to transmission and reception of a radar signal that travels through an ionospheric channel to a target located in free space. This corresponds to the situation of a long-range ground or space based radar. It is shown that aperture averaging can greatly affect measurements of scattering loss, signal decorrelation time, mean time delay and time delay jitter. Simple analytic expressions are given for all these quantities in terms of the geometry of the propagation path and the severity and structure of the ionization irregularities.

8

To obtain results applicable to a general geometry of the line-of-sight relative to the field aligned ionization structure, it is necessary to obtain an analytic solution for the two-position, two-frequency, mutual coherence function (MCF) for spherical wave propagation through a thick layer of anisotropic electron density irregularities. It is assumed here that strong scattering conditions prevail and that the quadratic approximation to the phase structure-function is valid.

This approximation was used by Sreenivasiah et al., (1976) and by Sreenivasiah and Ishimaru (1979) for the cases of plane wave and beam wave propagation in homogeneous turbulence. More recently the two-position, two-frequency mutual coherence function was obtained for spherical wave propagation using the extended Huygens-Fresnel principle (Fante, 1981). Although the quadratic structure-function approximation can sometimes lead to difficulties (Wandzura, 1980) it is appropriate for the two-frequency mutual coherence function but not for calculation of higher moments of the field (Fante, 1980). Fante (1981) discusses the accuracy of the quadratic structure-function approximation for the case of atmospheric turbulence with a Kolmogorov power spectrum. He has found that the accuracy is a function of the irregularity power spectrum and of the strength of the turbulence (Private Communication, 1982), with accuracy increasing for stronger scattering.

This aspect of the work here is a generalization of an earlier calculation (Knepp, 1983(b)) valid only for isotropic turbulence. As in the former study, the results here are specialized to the case of a thin phase-screen approximation to the thick scattering medium. With this simplification, analytic results are obtained for the received impulse response function to a transmitted power delta function. Then results may

9

easily be determined for the mean time delay and time delay jitter for strong, anisotropic turbulence in the thin phase-screen approximation. Results for these quantities in this approximation have previously been shown (Knepp, 1983(b)) to closely approximate the results for a thick scattering layer for the case of isotropic turbulence.

The effects of Gaussian antennas on measurements of received power, decorrelation time (or distance), mean time delay, time delay jitter and coherence bandwidth are determined. It is shown that aperture averaging can reduce observed signal power, increase observed decorrelation time and be a significant factor in reduced observed time-of-arrival jitter at the antenna output.

SECTION 2
FORMULATION

In this section the solution for the two-position, two-frequency mutual coherence function is presented for transmitter and receiver located on opposite sides of a thick layer of anisotropic electron density irregularities. In the next section this result is utilized to determine the effect of transmitting and receiving antennas on measurements of the received signal.

Consider a monochromatic spherical wave $E(\overline{\rho},z,\omega,t)$ which originates from a transmitter located at $(0,0,-z_t)$ and propagates in free space in the positive z direction where it is incident on an ionization irregularity layer which extends from $0 \le z \le L$. After emerging from the layer at $z = L$, the wave then propagates in free space to a receiver located at $(0,0,z_r)$. This thick layer geometry is shown in Figure 1. As the wave propagates, its phase substantially behaves as $(-i<k>z+i\omega t)$ so write

$$E(\overline{\rho},z,\omega,t) = U(\overline{\rho},z,\omega) \exp\left\{i\left(\omega t - \int <k(z')>dz'\right)\right\} \qquad (1)$$

where $<k(z)>$ is the mean wave number given by

$$<k(z)> = \frac{\omega}{c} \left(1 - N_e/n_c\right)^{1/2} = k \left(1 - k_p^2/k^2\right)^{1/2} \qquad (2)$$

where c is the speed of light in a vacuum, N_e is the mean ionization density, n_c is the critical electron density and is related to the classical electron radius r_e by $n_c = \pi/(\lambda^2 r_e)$, $(r_e = 2.82\times10^{-15}$ m).
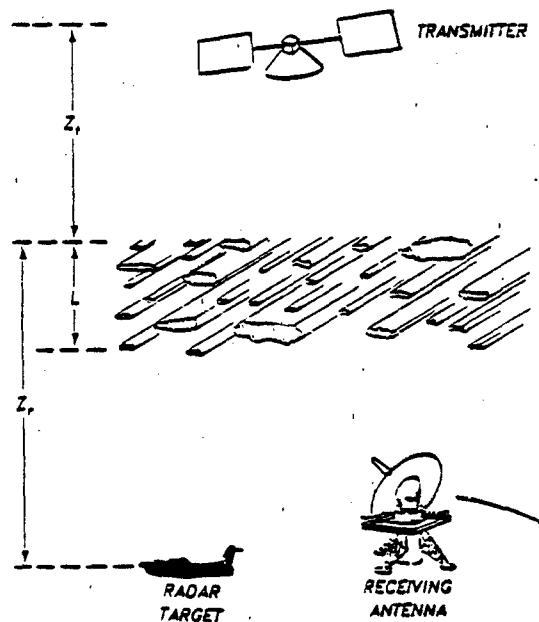
Figure 1. Propagation of signals through a disturbed
transionospheric channel.

In the case that the transmitted waveform is no longer a mono-
chromatic wave, but can be expressed as a waveform modulated on a carrier,
the two-position, two-frequency MCF Γ is of interest. Γ is important
for the calculation of pulse propagation in a random medium and it serves
as a basis from which to calculate the important power impulse response
function and its moments. Under the Markov approximation, Γ is found to
satisfy (Yeh and Liu, 1977; Knepp, 1983(b)).

$$\frac{\partial \Gamma}{\partial z} - \frac{i}{2(k_s^2 - k_d^2/4)} [k_d \nabla_d^2 + \frac{1}{4} k_d \nabla_s^2 - 2k_s \nabla_s \cdot \nabla_d] \Gamma$$

$$- \frac{1}{8} \left[\frac{2k_p^4}{k_1 k_2} A(\varsigma, \eta) - \left(\frac{1}{k_1^2} + \frac{1}{k_2^2} \right) k_p^* A(0) \right] \Gamma = 0 \qquad (3)$$

where ∇_s and ∇_d are the gradient operators in the sum and difference coordinate system. Here $\Gamma = \langle U(x_1,y_1,z,\omega_1)U^*(x_2,y_2,z,\omega_2)\rangle$ which is written as $\Gamma(\zeta,n,z,\omega_d)$ after the sum and difference transformation. The standard transformations

$$x = (x_1+x_2)/2 \qquad \zeta = x_1-x_2$$

$$Y = (y_1+y_2)/2 \qquad n = y_1-y_2$$

$$k_s = (k_1+k_2)/2 \qquad k_d = k_1-k_2$$

are used to obtain Equation 3. In addition, it has been assumed that the frequencies of interest are much greater than the plasma frequency. The quantity k_s is the wavenumber at the carrier frequency, $k_s = \omega_0/c$.

The function $A(\overline{\rho})$ is the integral of the autocorrelation function of electron density fluctuations, B_ξ, in the direction of propagation

$$A(\overline{\rho}_1-\overline{\rho}_2) = \int_{-\infty}^{\infty} B_\xi(\overline{\rho}_1-\overline{\rho}_2,z')dz' \tag{4}$$

where $\overline{\rho}_1-\overline{\rho}_2 = (x_1-x_2,y_1-y_2)$ and $\xi = \Delta N_e/\langle N_e\rangle$ so that

$$A(\overline{\rho}_1-\overline{\rho}_2) = 2\pi \int_{-\infty}^{\infty}\int \exp\left[i\overline{K}_\perp\cdot(\overline{\rho}_1-\overline{\rho}_2)\right] \phi_\xi(\overline{K}_\perp,K_z=0)d^2K_\perp \tag{5}$$

where ϕ_ξ is the power spectrum of electron density fluctuations. Equations 4 and 5 depend upon the validity of the Markov approximation where it is assumed that the electron density fluctuations are delta-correlated in the direction of propagation (Fante, 1975). That is $B_\xi(\overline{\rho}_1-\overline{\rho}_2,z_1-z_2) = A(\overline{\rho}_1-\overline{\rho}_2)\delta(z_1-z_2)$.

13

The unknown two-frequency MCF may be written as $\Gamma = \Gamma_1\Gamma_0$ (Knepp, 1983(b)) where Γ_0 is the exact free space solution in the parabolic approximation. Substitution of $\Gamma = \Gamma_1\Gamma_0$ into Equation 3 and neglect of near-zone terms yields a differential equation with terms containing the factors $\partial\Gamma_1/\partial X$ and $\partial\Gamma_1/\partial Y$. Since the boundary condition at $z = 0$, $\Gamma_1(\zeta,\eta,z=0,\omega_d) = 1$, is independent of X and Y, the derivatives with respect to these quantities may be neglected. The change of variables $z' = z + z_t$, $\theta = \zeta/z'$, $\phi = \eta/z'$, and the additional substitution $\Gamma_1 = \Gamma_2\Gamma_3$ where

$$\Gamma_3 = \exp\left\{ -\frac{1}{8} A(0)(z'-z_t)k_p^4\left(\frac{1}{k_1} - \frac{1}{k_2}\right)^2 \right\} \tag{6}$$

and the replacements

$$a = \frac{1}{2} k_d/k_s^2 \tag{7a}$$

$$b = \frac{1}{4} k_p^4/k_s^2 \tag{7b}$$

$$\nu = (abA_2)^{1/2} z' = a_1 z' \tag{8a}$$

$$\mu = \left(\frac{1}{a^3 bA_2}\right)^{1/4} \theta = a_2\theta \tag{8b}$$

$$\epsilon = \left(\frac{1}{a^3 bA_2}\right)^{1/4} \phi = a_2\phi \tag{8c}$$

enable one to write the equation for Γ_2 as

$$\frac{\partial\Gamma_2}{\partial\nu} - i \frac{1}{\nu^2}\left(\frac{\partial^2}{\partial\mu^2} + \frac{\partial^2}{\partial\epsilon^2}\right)\Gamma_2 - (\mu^2 + \Delta^2\epsilon^2)\nu^2\Gamma_2 = 0 \tag{9}$$

14

where $A(\zeta,\eta)$ has been expanded in a truncated Taylor series

$$A(\zeta,\eta) = A_0 + A_2\zeta^2 + \Delta^2 A_2\eta^2 \tag{10}$$

(see appendix). This is the quadratic phase structure function approximation. The difference wave number k_d has also been neglected with respect to k_s. The effect of this assumption is to restrict the validity of the solution to a small range of wavelengths centered about k_s.

Thick Layer Solution

An analytic solution of the form

$$\Gamma_2 = f(\nu) \exp\{-g(\nu)\mu^2 - h(\nu)\epsilon^2\} \tag{11}$$

may be substituted into Equation 9 to obtain three equations, the first consisting of terms that are factors of μ^2, the second consisting of factors of ϵ^2, and the third independent of μ and ϵ. These equations may be solved exactly for Γ_2, and the results substituted into Equation 3 to yield

$$\Gamma_1(\theta,\phi,z'=L+z_t,\omega_d) =$$

$$F \exp\{-(A-\beta t)\theta^2 - (A-\Delta\beta t')\phi^2\} \tag{12}$$

where

$$F = \exp\left\{-\frac{\sigma_\phi^2 \omega_d^2}{2\omega_0^2}\right\} \beta a_1(L+z_t)$$

$$\times \left[\frac{\Delta}{(\beta a_1 z_t \cosh \beta a_1 L + \sinh \beta a_1 L)(\Delta\beta a_1 z_t \cosh \Delta\beta a_1 L + \sinh \Delta\beta a_1 L)}\right]^{1/2} \tag{13}$$

$$A = \frac{i(L+z_t)\, a_1 a_2^2}{4} \tag{14}$$

$$B = \frac{(L+z_t)^2\, a_1^2 a_2^2}{\beta} \tag{15}$$

$$t = \frac{1 + \beta a_1 z_t \tanh \beta a_1 L}{\beta a_1 z_t + \tanh \beta a_1 L} \tag{16}$$

$$t' = \frac{1 + \Delta\beta a_1 z_t \tanh \Delta\beta a_1 L}{\Delta\beta a_1 z_t + \tanh \Delta\beta a_1 L} \tag{17}$$

$$\beta^2 = -i4 \tag{18}$$

In transcribing Equation 6 for Γ_3, the relationship between the coefficient A_0 and the phase variance σ_ϕ^2 given by Equation A-6a is utilized. Equation A-5 gives the expression for the quantity Δ in terms of the geometry of the line-of-sight relative to the magnetic field direction.

To complete the solution, it is necessary to solve for Γ_1 in the region $L \leq z \leq z_r$ (see Figure 1). Equation 12 serves as the boundary condition at $z' = L + z_t$. Since the region $z' \geq L + z_t$ corresponds to free space with no ionization, Equation 3 is appropriate after the Γ_0 substitution is included, insertion of the z', θ, and ϕ substitutions, and deletion of the last term involving the function A that is zero in free space.

The Fourier transform

$$\Gamma_1(\theta,\phi,z',\omega_d) = \int_{-\infty}^{\infty} \int_{-\infty}^{\infty} e^{i(K_\theta\theta+K_\phi\phi)}$$

$$x \quad \hat{\Gamma}_1(K_\theta,K_\phi,z',\omega_d) \; dK_\theta dK_\phi \tag{19}$$

may be substituted into the suitably modified Equation 3 to obtain the algebraic equation

$$\frac{\partial\hat{\Gamma}_1}{\partial z'} + \frac{i}{2}\frac{k_d}{k_s^2}\frac{1}{z'^2}(K_\theta^2 + K_\phi^2)\hat{\Gamma}_1 = 0 \tag{20}$$

Equation 20 may be solved, and the boundary condition Equation 12 applied at $z' = L + z_t$ with the result

$$\hat{\Gamma}_1(K_\theta,K_\phi,z_t+z_r,\omega_d) = \hat{\Gamma}_1(K_\theta,K_\phi,L+z_t,\omega_d)$$

$$x \; \exp\left[-i\gamma(K_\theta^2 + K_\phi^2)\right] \tag{21}$$

where

$$\gamma = \frac{1}{2}\frac{k_d}{k_s^2}\frac{(z_r-L)}{(L+z_t)(z_t+z_r)} \tag{22}$$

The final result may then be obtained by taking the Fourier transform of Equation 12 to obtain $\hat{\Gamma}_1(K_\theta,K_\phi,z_t+z_r,\omega_d)$ and then taking the inverse Fourier transform of Equation 21. The required integrals are easily found, and the result may be written as

$$\Gamma_1(\zeta,\eta,z_t+z_r,\omega_d) = \frac{F}{[(1+i4\gamma(A-Bt))\ (1+i4\gamma(A-\Delta Bt'))]^{1/2}}$$

$$\times \exp\left\{-\frac{\zeta^2(A-Bt)/(z_t+z_r)^2}{1+i4\gamma(A-Bt)} - \frac{\eta^2(A-\Delta Bt')/(z_t+z_r)^2}{1+i4\gamma(A-\Delta Bt')}\right\} \qquad (23)$$

Equation 23 is the result for Γ_1 after propagation through a thick layer characterized by anisotropic electron density irregularities. The full solution for the two-position, two-frequency MCF is obtained by multiplication by Γ_0, the free space MCF. Since Γ_0 is not affected by the random layer, it may be ignored here.

Thin Phase-Screen Approximation

Much simplification is possible if the thick scattering layer is replaced by an equivalent thin phase-screen of infinitesimal thickness and the same overall phase variance. To the first order, in the thin phase-screen approximation

$$\cosh \Delta\alpha a_1 L \approx 1 \qquad (24a)$$

$$\sinh \Delta\alpha a_1 L \approx \Delta\alpha a_1 L \qquad (24b)$$

$$\tanh \Delta\alpha a_1 L \approx \Delta\alpha a_1 L \qquad (24c)$$

Utilizing these approximations as well as Equations 8a-c and Equation 18 for a_1, a_2, and β, the two-position, two-frequency MCF is found in the thin phase-screen limit as

$$\Gamma_1(\xi,\eta,z_t+z_r,\omega_d) \simeq \left[\frac{1}{\left(1+i\ \frac{\omega_d}{\omega'}\right)\left(1+i\ \frac{\omega_d}{\omega'/\Delta^2}\right)}\right]^{1/2}$$

$$\times \exp\left\{-\ \frac{\sigma_\phi^2\ \omega_d^2}{2\omega_0^2}\right\} \exp\left\{-\ \frac{\zeta^2/\ell_0^2}{1+i\ \frac{\omega_d}{\omega'}} - \frac{\eta^2/(\ell_0^2/\Delta^2)}{1+i\ \frac{\omega_d}{\omega'/\Delta^2}}\right\} \qquad (25)$$

where

$$\ell_0^2 = -\ \frac{(z_t+z_r)^2 A_0}{z_t^2 \sigma_\phi^2 A_2} \qquad (26)$$

$$\omega' = -\ \frac{\pi\omega_0(z_t+z_r)A_0}{\lambda z_r z_t \sigma_\phi^2 A_2} \qquad (27)$$

Equations 25-27 are valid for any anisotropic power spectrum for which, in the strong scattering limit, the phase structure-function can be expanded in the form of Equation 10. For the anisotropic Gaussian power spectrum of interest in this work $A_0/A_2 = -r_0^2$ where r_0 is the axial scale size of the elongated irregularities as discussed in the appendix. The parameter ℓ_0 is a measure of the decorrelation distance of the complex electric field as measured in the plane of the receiver; ω' is the coherence bandwidth and will be shown to be inversely proportional to the time delay jitter; σ_ϕ is given in the appendix as the phase standard deviation imposed on the wave by the phase-screen.

19

SECTION 3
APERTURE ANTENNA EFFECTS

In this Section, appropriate expressions are derived to obtain
the effect of the antenna aperture on measurements of the properties of
the received signal during strong scintillation conditions. The first
geometry considered is that of a spherical wave that propagates through
the disturbed layer to a receiving aperture antenna. Results for this
case are then easily extended to the case of a transmitting and receiving
antenna and then to the case of a monostatic radar geometry.

Consider the geometry shown in Figure 2 where the aperture is
located in the receiver plane, $z = z_r$. If the incident field in the
plane of the antenna is $U(\bar{\rho}, z_r, \omega)$, then the complex voltage envelope at
the antenna output may be expressed as (Price, Chesnut and Burns, 1972)

$$v(\bar{\rho}_0, z_r, \omega) = \int U(\bar{\rho}', z_r, \omega) \, A_r^*(\bar{\rho}' - \bar{\rho}_0) \, d^2\rho' \qquad (28)$$

where U is the solution to the parabolic wave equation at location $\bar{\rho}'$
in the receiver plane for a monochromatic signal of frequency ω, $\bar{\rho}_0$ is
the location of the center of the aperture antenna and A_r^* is the complex
antenna weighting function.

Equation 28 gives the output voltage from an aperture antenna
pointed in the z-direction for a transmitted monochromatic waveform of
radian frequency ω. If the transmitted waveform is a pulse waveform
modulated on a carrier, the transmitted signal can be expressed as

$$s(\tau) = \text{Re}\left\{ m(\tau) \exp(i\omega_0 \tau) \right\} \qquad (29)$$
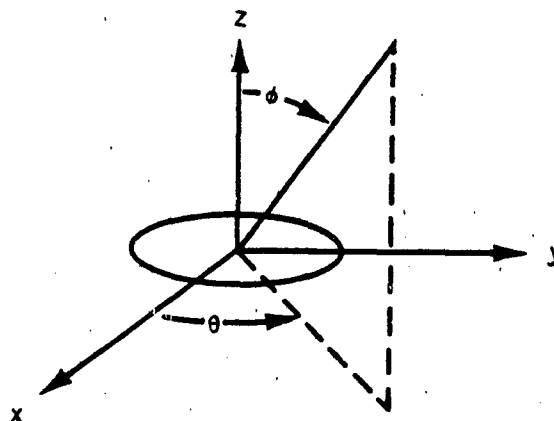
Figure 2. Receiving antenna aperture centered at origin of coordinate system.

where ω_0 is the carrier radian frequency and $m(\tau)$ is the modulation waveform. After passage through a layer of irregularities, the received signal may be written (Knepp, 1983(a)) in the absence of an antenna, as

$$r(\overline{\rho},z_r,\tau) = \text{Re}\left\{e(\overline{\rho},z_r,\tau)\exp(i\omega_0\tau)\right\} \qquad (30)$$

where

$$e(\overline{\rho},z_r,\tau) = \frac{1}{2\pi}\int_{-\infty}^{\infty} M(\omega)U(\overline{\rho},z_r,\omega+\omega_0)\exp(i\omega\tau)d\omega \qquad (31)$$

The quantity e is called the complex envelope of the received waveform. $M(\omega)$ is the Fourier transform of the transmitted modulation waveform and is given by

$$M(\omega) = \int_{-\infty}^{\infty} m(\tau)\exp(-i\omega\tau)d\tau \qquad (32)$$

21

In order to obtain the effect of the antenna on the received time-domain waveform, the received complex envelope U in Equation 31 is replaced by the expression for v given by Equation 28. Thus the received time-domain signal at the antenna output may be written as

$$e(\overline{\rho}_0, z_r, \tau) = \frac{1}{2\pi} \int M(\omega) U(\overline{\rho}', z_r, \omega+\omega_0)$$

$$\times A_r^*(\overline{\rho}'-\overline{\rho}_0) \exp(i\omega\tau) d^2\rho' d\omega \quad (33)$$

In the case that the receiving aperture is an omnidirectional point antenna, A^* is a delta function and the received complex envelope given by Equation 33 is identical to the result given by Equation 31.

For the case that the transmitted signal power has a delta function behavior in delay, $m(\tau)m^*(\tau) = \delta(\tau)$, the correlation function of the received power can be expressed as

$$\langle e(\overline{\rho}_1, z_r, \tau) e^*(\overline{\rho}_2, z_r, \tau) \rangle = G(\overline{\rho}_1 - \overline{\rho}_2, \tau)$$

$$= (2\pi)^4 \int S(\overline{K}, \tau) \left| A_r(\overline{K}) \right|^2 \exp\left[i\overline{K}\cdot(\overline{\rho}_1-\overline{\rho}_2)\right] d^2K \quad (34)$$

where $S(\overline{K}, \tau)$ is the generalized power spectrum (Knepp and Wittwer, 1984) defined as the Fourier transform of the MCF,

$$S(\overline{K}, \tau) = \frac{1}{8\pi^3} \int \Gamma(\overline{\rho}_d, \omega_d) \exp(-i\overline{K}\cdot\overline{\rho}_d + i\omega_d\tau) d\omega_d d^2\rho_d \quad (35)$$

and $A_r(\overline{K})$ is the Fourier transform of the weighting function of the receiving aperture

$$A_r(\overline{K}) = \frac{1}{4\pi^2} \int A_r(\overline{\rho}) \exp(-i\overline{K}\cdot\overline{\rho}) d^2\rho \quad (36)$$

22

The vector $\overline{K}$ is given as $k \sin\theta(\cos\phi \,\hat{i} + \sin\phi \,\hat{j})$ for the geometry shown in Figure 2.

To obtain Equation 34, use is made of the fact that the MCF depends on only the differences in position and frequency. A detailed derivation similar to the above appears in Ishimaru (1978). Note that the dependence of the power impulse response function, G, on the receiver distance z_r has been omitted for notational convenience.

Equation 34 can be written in another very useful form with the substitution

$$\hat{\Gamma}(\overline{K},\omega_d) = \frac{1}{4\pi^2} \int \Gamma(\overline{\rho}_d,\omega_d)\exp(-i\overline{K}\cdot\overline{\rho}_d)d^2\rho_d \tag{37}$$

where $\hat{\Gamma}(\overline{K},\omega_d)$ is the Fourier transform of the MCF. If $\hat{\Gamma}$ is used in Equation 34 one obtains

$$G(\overline{\rho}_1-\overline{\rho}_2,\tau) = (2\pi)^3 \int \hat{\Gamma}(\overline{K},\omega_d)\left|A_r(\overline{K})\right|^2 \exp\left[i\overline{K}\cdot(\overline{\rho}_1-\overline{\rho}_2)+i\omega_d\tau\right]d\omega_d d^2K \tag{38}$$

It will be seen that Equation 38 is preferable for the evaluation of the effects of apertures on mean time delay and time delay jitter.

For later usage, it is noted that the function $\hat{\Gamma}(\overline{K},\omega_d)$ may be obtained directly from Equation 25 as

$$\hat{\Gamma}(\overline{K},\omega_d) = \frac{\ell_o^2}{4\pi\Delta} \exp\left\{-\frac{\sigma_\phi^2\omega_d^2}{2\omega_o^2}\right\}$$

$$\times \exp\left\{-\frac{K_x^2\ell_o^2}{4}\left(1+i\frac{\omega_d}{\omega'}\right)-\frac{K_y^2\ell_o^2}{4\Delta^2}\left(1+i\frac{\omega_d}{\omega'/\Delta^2}\right)\right\} \tag{39}$$

Aperture Weighting Function

Let the antenna possess a Gaussian beam pattern with gain function

$$G(\theta) = G_0 \exp\left(-\theta^2/\theta_r^2\right) \qquad (40)$$

where the receiver beamwidth θ_r is related to the effective aperture diameter D by $\theta_r^2 = (\lambda/D)^2/(4\ln 2)$ and λ is the wavelength at the carrier frequency. With this choice of beamwidth $G(\lambda/2D) = G_0/2$ so that this Gaussian aperture has approximately the same 3 dB beamwidth as a uniformly illuminated circular antenna. The antenna gain pattern is the square of the transform of the aperture response function defined earlier. Thus

$$A_r(\overline{K}) = G_0^{1/2} \exp\left(-\theta^2/2\theta_r^2\right) \qquad (41)$$

The Fourier transform relationship of Equation 36 may be used and the small angle approximation invoked to obtain the aperture weighting function and its Fourier transform as

$$A_r(\overline{\rho}) = 2\pi k_0^2 \theta_0^2 G_0^{1/2} \exp\left(-k^2\rho^2\theta_r^2/2\right) \qquad (42)$$

and

$$A_r(\overline{K}) = G_0^{1/2} \exp\left(-K^2/2k^2\theta_r^2\right) \qquad (43)$$

Before proceeding, it is useful to note that the effect of an aperture antenna is immediately apparent from the form of Equation 38. With a point or omnidirectional antenna, the beamwidth is large in Equation 43 and $A_r(\overline{K})$ is constant. Therefore, with a point antenna, the aperture angular response function is not important in Equation 38. It is apparent that the receiving aperture acts to modify the value of $\hat{\Gamma}$ such that

$$\hat{\Gamma}_a(\overline{K},\omega_d) = \hat{\Gamma}_r(\overline{K},\omega_d)\left|A_r(\overline{K})\right|^2 \qquad (44)$$

24

where the subscript a on $\hat{\Gamma}$ denotes that this expression contains the effect of the receiving aperture. The subscript r on $\hat{\Gamma}$ on the right hand side of Equation 44 refers to the case here that the receiver is located at z_r. This equation is an explicit expression of the well known result that an aperture modifies the angular spectrum of the received signal.

Case of Transmitting and Receiving Antennas

Equations 34 and 38 give the received power impulse response function for the case of an omnidirectional spherical wave transmitter and a receiving aperture antenna with aperture angular response function $A_r(\overline{K})$. A transmitting aperture antenna is easily included in Equations 34 and 38 since its only effect is to reduce the region of the phase-screen that is illuminated. This is accomplished by including an additional antenna angular response function $A_t(\overline{K}z_r/z_t)$ where $A_t(\overline{K})$ is the response function of the transmitter with beamwidth θ_t and where the factor z_r/z_t transforms the antenna angle utilized by the transmitter to the angle observed by the receiver. This transformation is equivalent to the observation that a ray transmitted from location $-z_t$ at the angle θ and that scatters from the thin layer is observed by the receiver at angle $\theta' = z_t\theta/z_r$. For this case one may write

$$\hat{\Gamma}_{tr}(\overline{K},\omega_d) = \hat{\Gamma}_r(\overline{K},\omega_d)\left|A_r(\overline{K})\right|^2 \left|A_t(\overline{K}z_r/z_t)\right|^2 \tag{45}$$

where the subscript tr refers to the fact that this expression includes the effects of both transmitting and receiving apertures. Since the one-way propagation path here again utilizes a receiver at z_r, $\hat{\Gamma}$ on the right hand side again appears with the subscript r.

For the later calculations of scattering loss, mean time delay and time delay jitter, Equation 38 is evaluated at $\bar{p}_1 - \bar{p}_2 = 0$ where Equation 45 is substituted for the factors $\hat{\Gamma}(\bar{K}, \omega_d)|A_r(\bar{K})|^2$. That is, for the one-way propagation path with both transmit and receive apertures

$$G_{tr}(0, \tau) = (2\pi)^3 \int \hat{\Gamma}_{tr}(\bar{K}, \omega_d) \exp(i\omega_d\tau) \, d^2K d\omega_d \qquad (46)$$

For evaluation of the effect of an aperture antenna on the measured signal decorrelation distance, the necessary function is the two-position, single frequency MCF given by the Fourier transform of Equation 37 as

$$\Gamma(\bar{p}_d, 0) = \int \hat{\Gamma}_{tr}(\bar{K}, 0) \exp(i\bar{K} \cdot \bar{p}_d) d^2K \qquad (47)$$

The use of $\hat{\Gamma}_{tr}$ includes the effect of both transmitting and receiving apertures.

Case Of Monostatic Radar

Now consider the case that the two-antenna geometry above is replaced by a monostatic radar geometry. In the radar case, the solution is facilitated by considering two one-way propagation paths. Let the radar antenna be located at $(0,0,-z_t)$ and also let the antenna angular response function be given by A_t with beamwidth θ_t on both transmission and reception. First consider the one-way propagation path from the transmitter antenna to the target located at $(0,0,z_r)$. For this path, the effect of the aperture antenna is obtained from Equation 45 with the omission of A_r, since the point target accepts energy incident from all directions. That is,

$$\hat{\Gamma}_{m1}(\bar{K}, \omega_d) = \hat{\Gamma}_r(\bar{K}, \omega_d)|A_t(\bar{K}z_r/z_t)|^2 \qquad (48)$$

where the subscript ml refers to the first one-way propagation path for the monostatic radar geometry.

Now consider the second one-way propagation path from the target back to the receiver. This is the propagation geometry initially considered in this report except for the interchange of receiver and transmitter location. For this one-way propagation path, $\hat{\Gamma}$ is replaced by $\hat{\Gamma}_t$ appropriate to the one-way propagation path from z_r to $-z_t$. Thus

$$\hat{\Gamma}_{m2}(\overline{K}, \omega_d) = \hat{\Gamma}_t(\overline{K}, \omega_d)|A_t(\overline{K})|^2 \qquad (49)$$

Note that the occurrence of A_t here as well as in Equation 48 signifies the use of the same aperture antenna (with beamwidth θ_t) for reception as well as transmission. The only effect of the reversal of the direction of propagation is an interchange of z_r and z_t in the calculation of the MCF. This interchange has the effect of replacing ℓ_o in Equation 39 with the term $\ell_o' = z_t \ell_o / z_r$.

In the case of the monostatic radar geometry under consideration, the principle of reciprocity states that the propagating signal takes the same path over each of the one-way propagation paths. This is true provided that the random medium is "frozen" for the duration of the signal traversal.

The power impulse response function for the signal received at the target due to a transmitted delta function of power from the radar is given by Equation 38 as

$$G_1(0, \tau) = (2\pi)^3 \int \hat{\Gamma}_{m1}(\overline{K}, \omega_d) \exp(i\omega_d \tau) d^2K d\omega_d \qquad (50)$$

If a delta function of power is transmitted from the target, the
power impulse response function at the radar receiver is given by a
similar expression

$$G_2(0,\tau) = (2\pi)^3 \int \hat{r}_{m2}(\overline{K},\omega_d)\exp(i\omega_d\tau)d^2Kd\omega_d \qquad (51)$$

The net power impulse response function after transmission of a delta
function from the antenna, scattering from the target, and propagation
over both of the one-way paths is given as the convolution (Ishimaru,
1978)

$$G_m(0,\tau) = \int G_1(0,t')G_2(0,\tau-t')dt' \qquad (52)$$

where the subscript m refers to the monostatic radar geometry. Using
the convolution theorem, it is easy to show that

$$G_m(0,\tau) = (2\pi)^7 \int \hat{r}_{m1}(\overline{K},\omega_d)d^2K \; \hat{r}_{m2}(\overline{K}',\omega_d)d^2K' \; \exp(i\omega_d\tau)d\omega_d \qquad (53)$$

This equation is the equivalent of Equation 46 for the case of the one-way
propagation path.

The above considerations apply to the calculation of the power
impulse response function $G_m(0,\tau)$ for the case of monostatic radar.
For this geometry the signal decorrelation distance is easily obtained as
a simplification of the previous development for the one-way propagation
path. For a monostatic radar, the decorrelation distance is obtained by
transmission of a signal to the target and observation of the scattered
signal at two spatial locations in the plane of the receiver. The point
target acts as a transmitter of a spherical wave which is then observed by

the radar receiver. For a small target and frozen irregularities, there is no dependence of signal decorrelation distance on the one-way propagation path from the transmitter to the target. The necessary two-position, single frequency MCF is given in a form similar to Equation 47 as

$$\Gamma(\overline{\rho}_d, 0) = \int \hat{\Gamma}'_{m2}(\overline{K}, 0) \exp(i\overline{K} \cdot \overline{\rho}_d) d^2K \tag{54}$$

where $\hat{\Gamma}_{m2}$ is given by Equation 49 and includes the effect of the receiving radar antenna. It will be shown that evaluation of the analytic form of the expression $\Gamma(\overline{\rho}_d, 0)$ immediately yields the signal decorrelation distance in this strong scatter calculation.

SECTION 4
RESULTS

In this section the derivations presented in Section 3 are utilized to obtain analytic expressions for several properties of the received signal as measured at the output of the appropriate aperture antenna.

Angular Scattering Loss

An antenna aperture acts to coherently collect the energy incident upon the antenna and to deliver it to the receiver. In the transmitting mode a directive antenna is designed to transmit energy only over a selected angular region. In the receiving mode this same directive antenna accepts energy only from a narrow range of angles. Thus, relative to an omnidirectional point antenna, a directive antenna will experience what is referred to as angular scattering loss when the signal at the aperture exhibits scintillation. This angular scattering loss arises from angle-of-arrival jitter present in the incident wavefront that may cause energy to arrive at the antenna propagating at angles greater than those accepted by the receiving aperture.

A different but equivalent way to view the effect of a receiving antenna aperture is as a coherent integrator of the signal arriving on the aperture face. If the antenna is pointing towards the source of an undisturbed plane wave, then the antenna output is maximum. If there are fluctuations in the signal phase across the aperture or the incident wavefront is tilted relative to the antenna boresight direction, the coherent integrator output is decreased.

It is convenient to compute the angular scattering loss as the ratio of the total power received with an antenna (or antennas) to that received with an omnidirectional antenna that experiences no loss. In both cases the transmitted signal power is taken as a delta function in delay. The angular scattering loss may be written as

$$
\text{loss} = \frac{\displaystyle\lim_{\theta_t, \theta_r \to \infty} \int G(0, \tau) d\tau}{\displaystyle\int G(0, \tau) d\tau} \tag{55}
$$

where the power impulse response function G is given by Equation 46 for the one-way path with both transmit and receive antennas and by Equation 52 for the monostatic radar case.

The integral of Equation 46 with respect to τ is easily evaluated using the identity $\int \exp(i\omega_d \tau) d\tau = 2\pi\delta(\omega_d)$. This leaves a two-dimensional integral of $\hat{\Gamma}(\overline{K}, 0)$ over angle which involves easily found integrals of Gaussian functions. The result may be written as

$$
\text{loss} = \left(1 + \frac{2\sigma_{\theta x}^2}{\theta_r^2} + \frac{2\sigma_{\theta x'}^2}{\theta_t^2}\right)^{1/2} \left(1 + \frac{2\sigma_{\theta y}^2}{\theta_r^2} + \frac{2\sigma_{\theta y'}^2}{\theta_t^2}\right)^{1/2} \tag{56}
$$

where $\sigma_{\theta x}$ and $\sigma_{\theta y}$ are the standard deviations of the theoretical angle-of-arrival fluctuations in the x- and y-directions over the propagation path from $-z_t$ to z_r. The quantities $\sigma_{\theta x'}$ and $\sigma_{\theta y'}$ are the same standard deviations calculated for the one-way propagation path from z_r to $-z_t$ (see appendix). The quantities θ_t and θ_r are the 3 dB beamwidths of the transmitting and receiving antennas, respectively.

The expression for angular scattering loss given by Equation 56 contains the effects of variations of the properties of the propagation medium and of the geometry of the propagation path. To show this result pictorially, let the antenna beamwidths be identical and let the equivalent phase-screen be located midway between transmitter and receiver. In this case $\ell_0' = \ell_0$. To simplify matters further, write the antenna beamwidth in terms of the diameter as discussed earlier. Write the angle-of-arrival jitter as a function of the signal decorrelation distance using the expressions given in the appendix. These substitutions give $2\sigma_{\theta x}^2/\theta_0^2 = 0.28\ D^2/\ell_0^2$ and $2\sigma_{\theta y}^2/\theta_0^2 = 0.28\ D^2/(\ell_0^2/\Delta^2)$. In order to separate the geometric effects of inclination angle variations from aperture averaging effects, define ℓ_p as the decorrelation distance for propagation parallel to the magnetic field line. The quantity ℓ_p is invariant with respect to changes in the inclination angle and is given from Equation 26 and A-6b by $\ell_p = \sqrt{\Delta}\ell_0$. The results remain a function of the axial ratio q which is here taken as 15 as suggested by Wittwer (1979).

Figures 3(a-b) show the angular scattering loss in decibels as a function of the relative antenna size D/ℓ_p and of the inclination angle. In Figure 3(a) the inclination angle between the magnetic field and the direction of propagation is shown for values of 0°, 15°, 30°, 45° and 90°. In Figure 3(b) the relative antenna size takes the values of 1, 3, 10, 30 and 100. It is seen in both figures that only when the antenna diameter is large with respect to the decorrelation distance is the angular scattering loss significant. Small inclination angles cause increased values of the observed phase standard deviation σ_ϕ and thus give increased angular scattering and increased scattering loss as shown. An increase in the inclination angle causes a decrease in σ_ϕ and an effective increase in the decorrelation distance ℓ_0; therefore, the amount of angular scattering loss decreases.
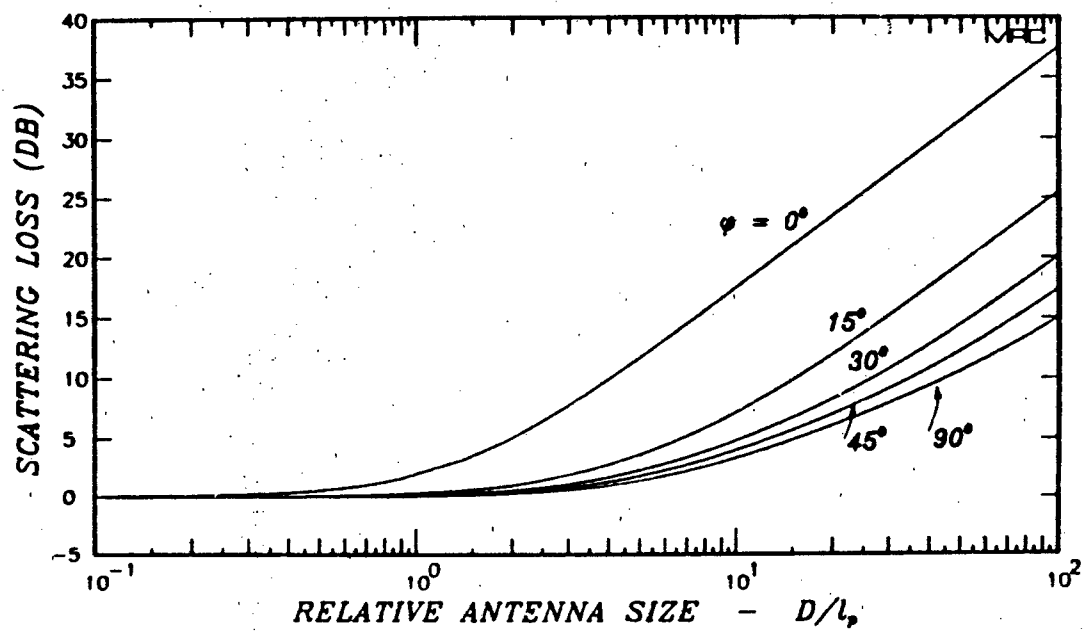
(a)
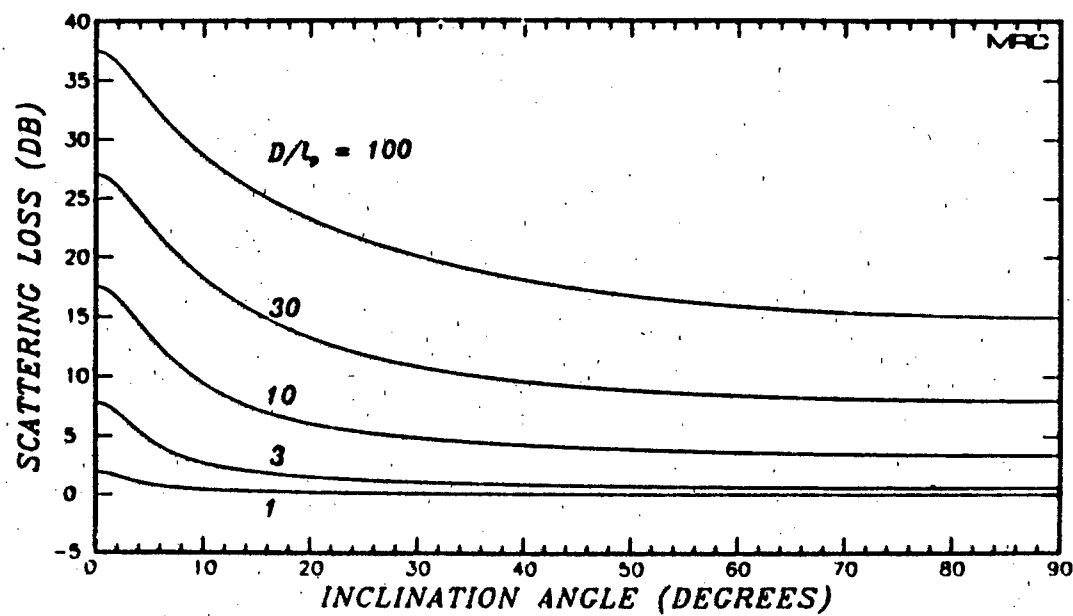
(b)

Figure 3.   Angular scattering loss for one-way path with transmit and
receive aperture antennas; a) versus relative antenna size;
b) versus inclination angle.

For the case of a monostatic radar, the power impulse response function is given by Equation 52 as the convolution of the power impulse response functions of each of the one-way propagation paths. A simple change of variables is utilized to reduce the integral $\int G_m(0,\tau)d\tau$ to the product of two integrals of G_1 and G_2. These integrals are easily performed using the delta function identity discussed previously with resulting angular scattering loss

$$\text{loss} = \left(1 + \frac{2\sigma_{\theta x'}^2}{\theta_t^2}\right)\left(1 + \frac{2\sigma_{\theta y'}^2}{\theta_t^2}\right) \tag{57}$$

where θ_t is the radar antenna 3 dB beamwidth. A comparison of this result to Equation 56 shows that the addition of a second one-way propagation path essentially squares the scattering loss.

Figures 4(a-b) show the angular scattering loss for the case of a monostatic radar geometry as a function of the inclination angle and of the relative antenna size D/ℓ_p. Here ℓ_p is the decorrelation distance observed for propagation parallel to the magnetic field along the path from $(0,0,z_r)$ to $(0,0,-z_t)$. The overall behavior of scattering loss is quite similar to that exhibited in Figure 3. The major difference observed is the increased loss caused by the additional one-way propagation path from the target back to the radar.

Signal Decorrelation Distance

As another aspect of the aperture averaging effect, an aperture can act to increase the measured decorrelation distance at the antenna output. This observed increase is caused by the averaging effect of the coherent integration that smooths the more rapid fluctuations. To obtain

34
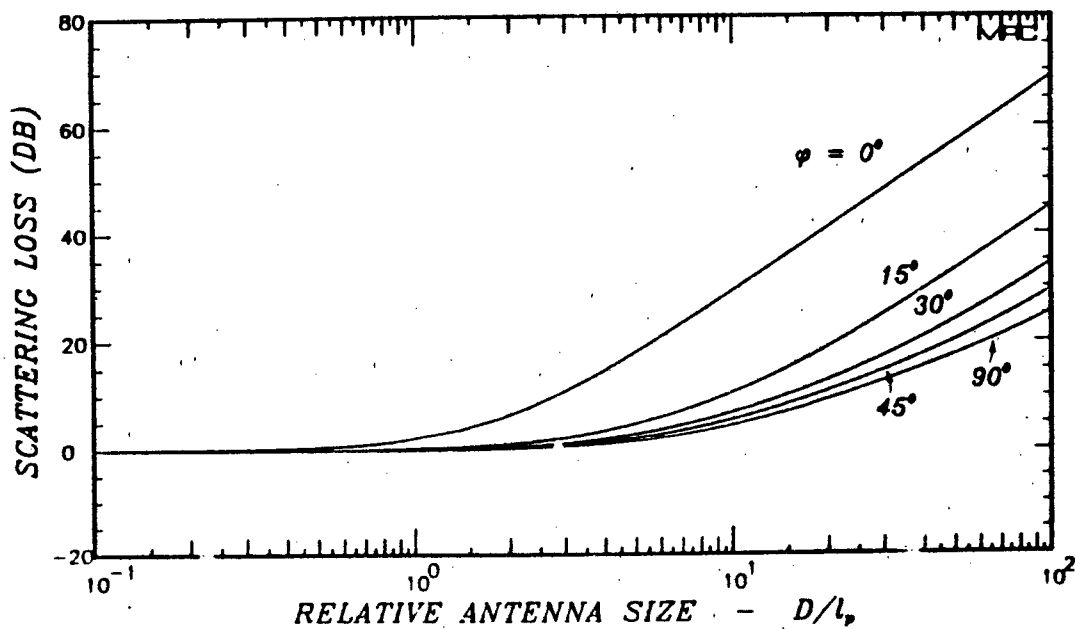
(a)
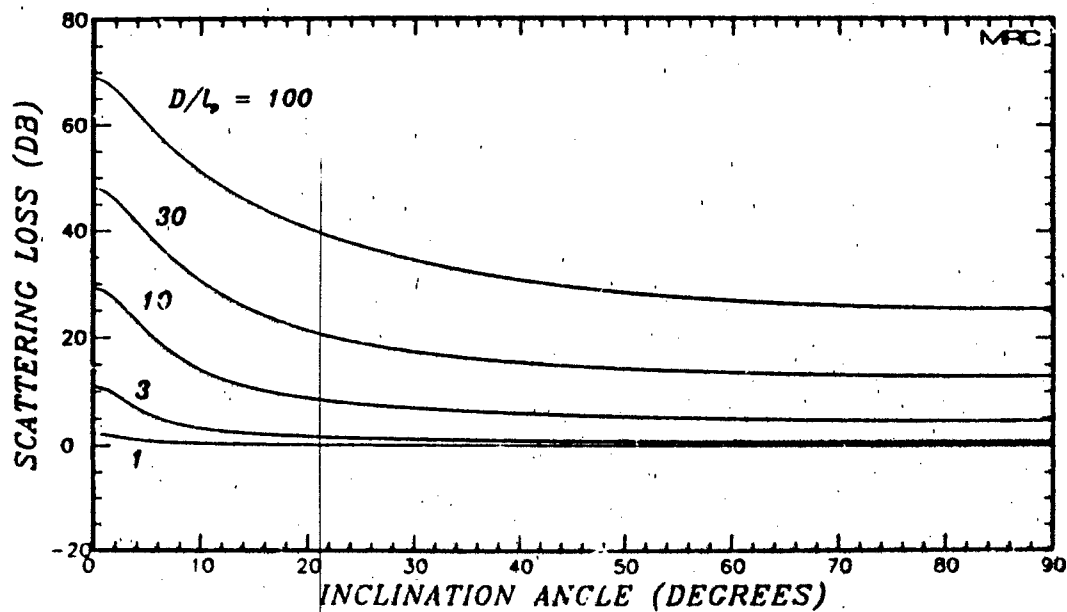
(b)

Figure 4.   Angular scatter loss for monostatic radar; a) versus
relative antenna size; b) versus inclination angle.

35

the signal decorrelation distance for the one-way propagation path from $(0,0,-z_t)$ to $(0,0,z_r)$, it is necessary to perform the integration specified in Equation 47. Fortunately, $\hat{\Gamma}$ given by Equation 45 is the product of simple Gaussian functions. The integral is available in standard tables and the resulting expression contains the factor $(-\zeta^2/\ell_{ox}^2 - \eta^2/\ell_{oy}^2)$ where the decorrelation distances in the x- and y-directions (see Figure A-1) are

$$\ell_{ox} = \ell_o\left(1 + \frac{2\sigma_{\theta x}^2}{\theta_r^2} + \frac{2\sigma_{\theta x'}^2}{\theta_t^2}\right)^{1/2} \tag{58}$$

$$\ell_{oy} = \frac{\ell_o}{\Delta}\left(1 + \frac{2\sigma_{\theta y}^2}{\theta_r^2} + \frac{2\sigma_{\theta y'}^2}{\theta_t^2}\right)^{1/2} \tag{59}$$

If small apertures are used so that the beamwidths are large with respect to the theoretical angle-of-arrival standard deviations, the parenthetical expressions above are unity leaving ℓ_{ox} and ℓ_{oy} in agreement with the coefficients of ζ and η given in Equation 25 with ω_d set to zero.

Figures 5 and 6 show the relative signal decorrelation distances ℓ_{ox}/ℓ_o and $\ell_{oy}/(\ell_o/\Delta)$ in the x- and y-directions for the case of identical transmit and receive antennas separated by a centrally located scattering layer. The quantities ℓ_o and ℓ_o/Δ are the values of decorrelation distance in the x- and y-directions, respectively, that are observed with omnidirectional antennas. In the figures the results are again shown as a function of the ratio of antenna diameter to the decorrelation distance for propagation parallel to the magnetic field direction.
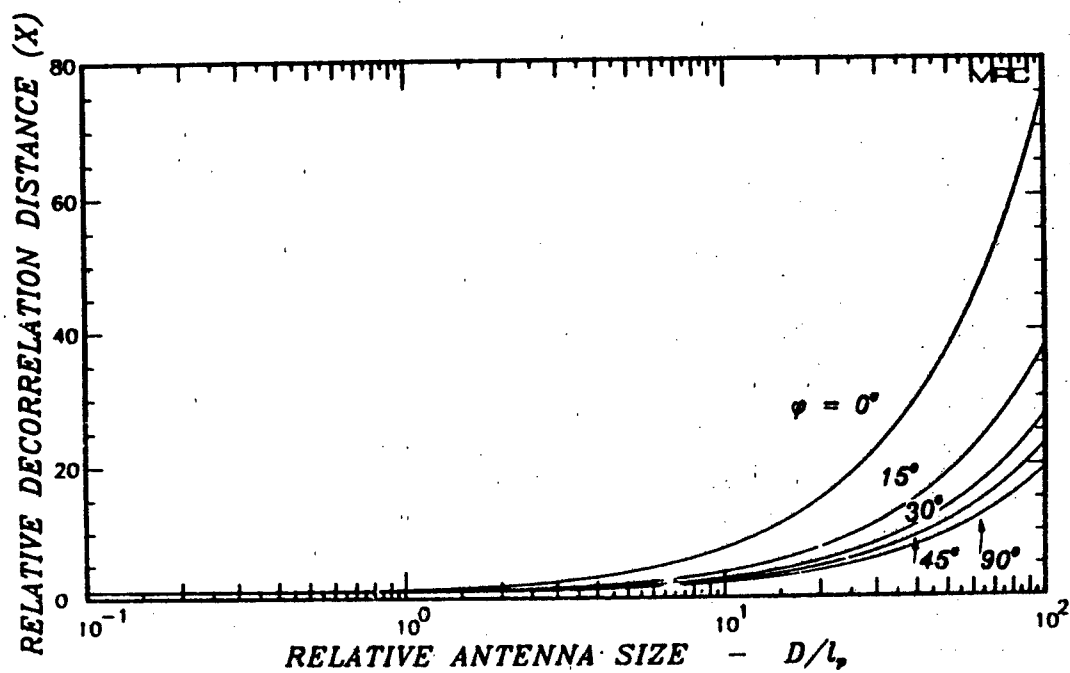
(a)
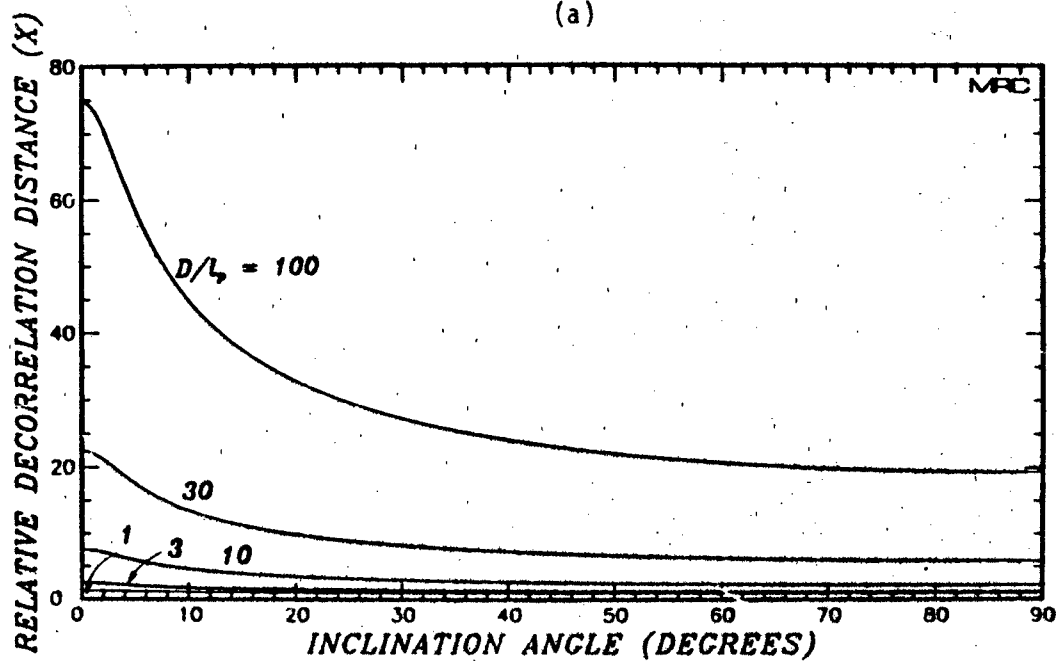
(b)

Figure 5.   Relative signal decorrelation distance in the x-direction
for one-way path with transmit and receive aperture
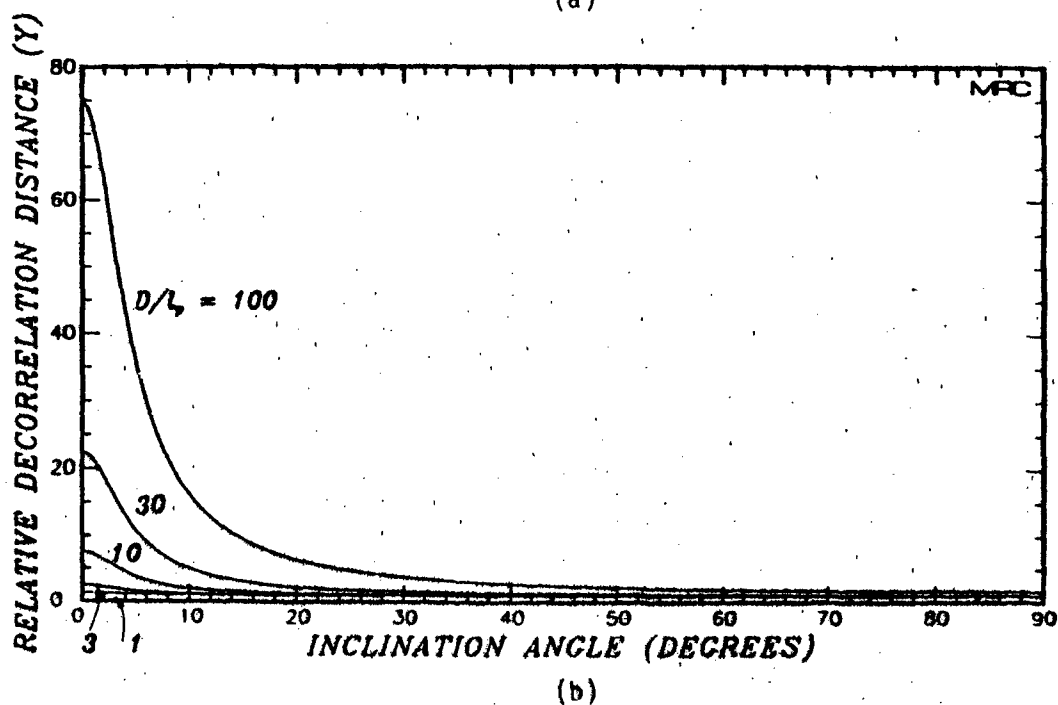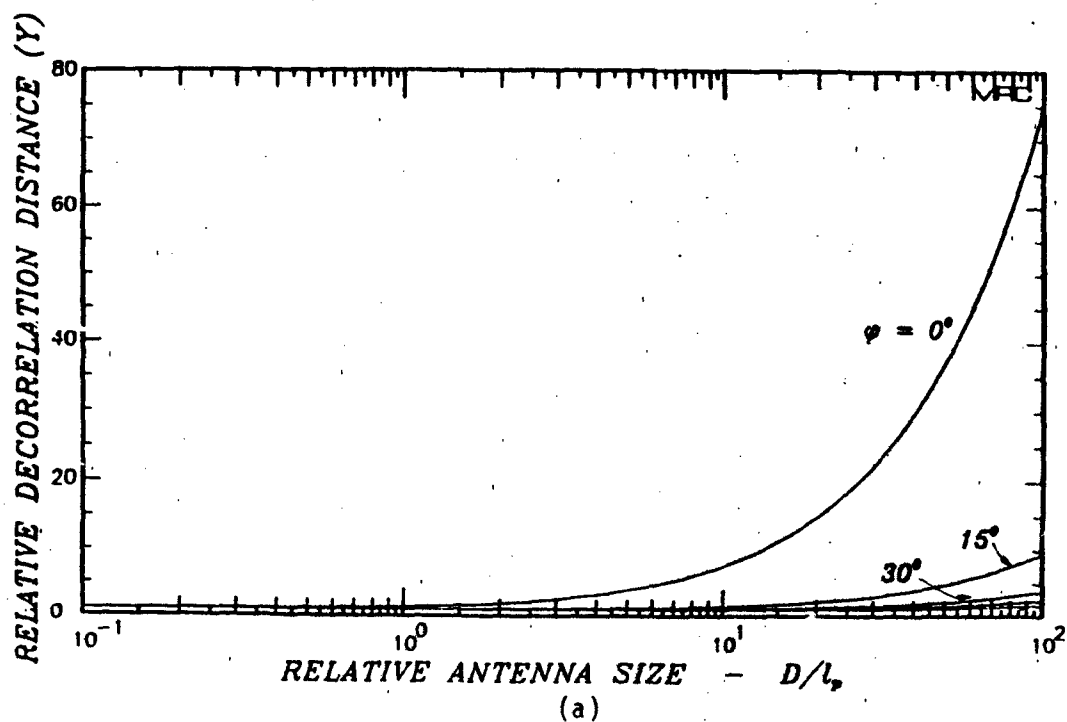antennas; a) versus relative antenna size; b) versus
inclination angle.

Figure 6.   Relative signal decorrelation distance in the y-direction
for one-way path with transmit and receive aperture
antennas; a) versus relative antenna size; b) versus
inclination angle.

Figures 5(a-b) show the relative decorrelation distance in the x-direction as functions of D/ℓ_p and inclination angle ψ. Apertures with diameters less than the decorrelation distance do not affect measurements of the signal decorrelation distance. It is evident that apertures large with respect to ℓ_p can greatly increase the measured decorrelation distance (relative to an omnidirectional antenna) for sufficiently strong angular scattering.

It is immediately evident that the decorrelation distance is not reciprocal. With omnidirectional antennas the decorrelation distances in the two orthogonal directions, ℓ_{ox} and ℓ_{oy}, are dependent on the path geometry as given by Equation 26. These values are not reciprocal; ℓ_{ox} and ℓ_{oy} are measures of the average distance between fades in the receiver plane and consequently depend on geometry.

In the case of the monostatic radar, the signal decorrelation distances may be obtained directly from Equations 58 and 59 by using the parameters appropriate to only the second one-way propagation path with transmitter (target) at $(0,0,z_r)$. The results are

$$\ell_{ox} = \ell_0' \left(1 + \frac{2\sigma_{\theta x'}^2}{\theta_\ell^2} \right)^{1/2} \tag{60}$$

$$\ell_{oy} = \frac{\ell_0'}{\Delta} \left(1 + \frac{2\sigma_{\theta y'}^2}{\theta_\ell^2} \right)^{1/2} \tag{61}$$

where ℓ_0' and ℓ_0'/Δ are the signal decorrelation distances in the x- and y- directions that correspond to the one-way propagation path from a source in the z_r plane to a receiver in the $-z_t$ plane. Figures 7-8 show ℓ_{ox} and ℓ_{oy} for a monostatic radar as a function of normalized antenna diameter and the angle between the magnetic field and the direction of propagation. The results are similar to those shown in Figures 5-6.

Figure 7.   Relative signal decorrelation distance in the x-direction for monostatic radar; a) versus relative antenna size; b) versus inclination angle.

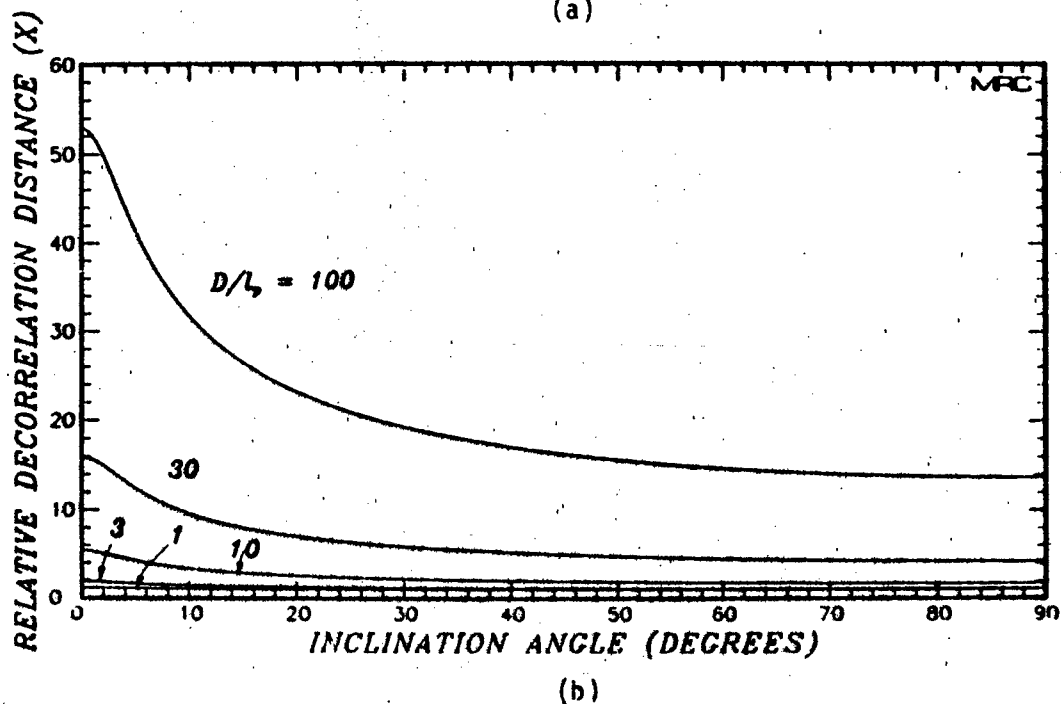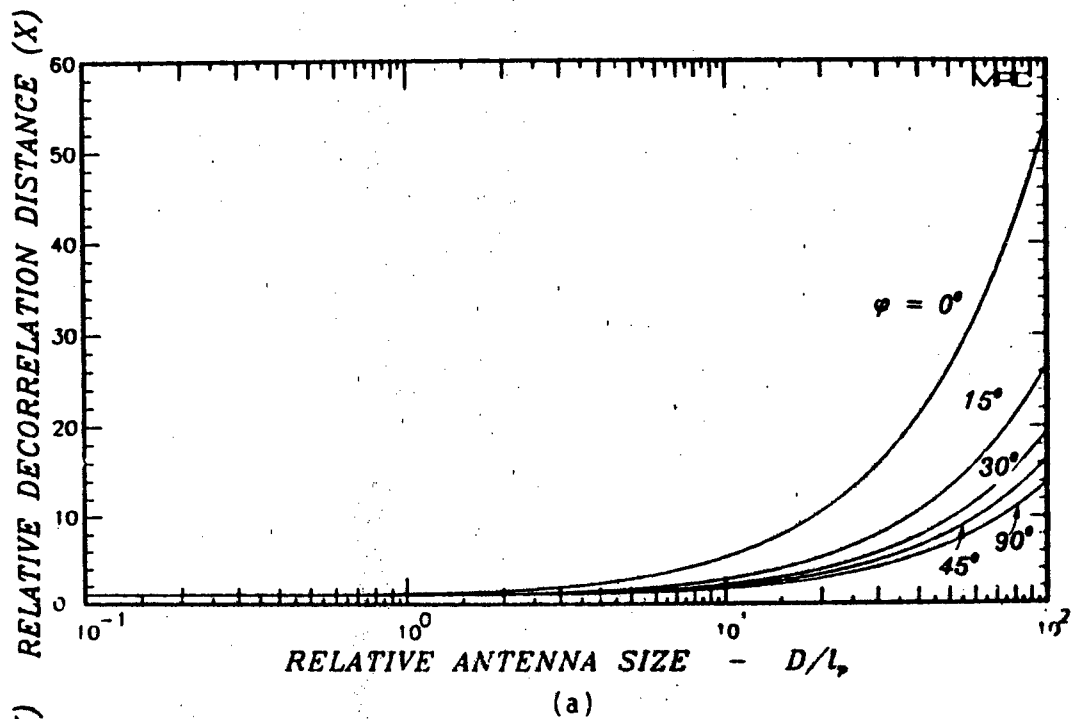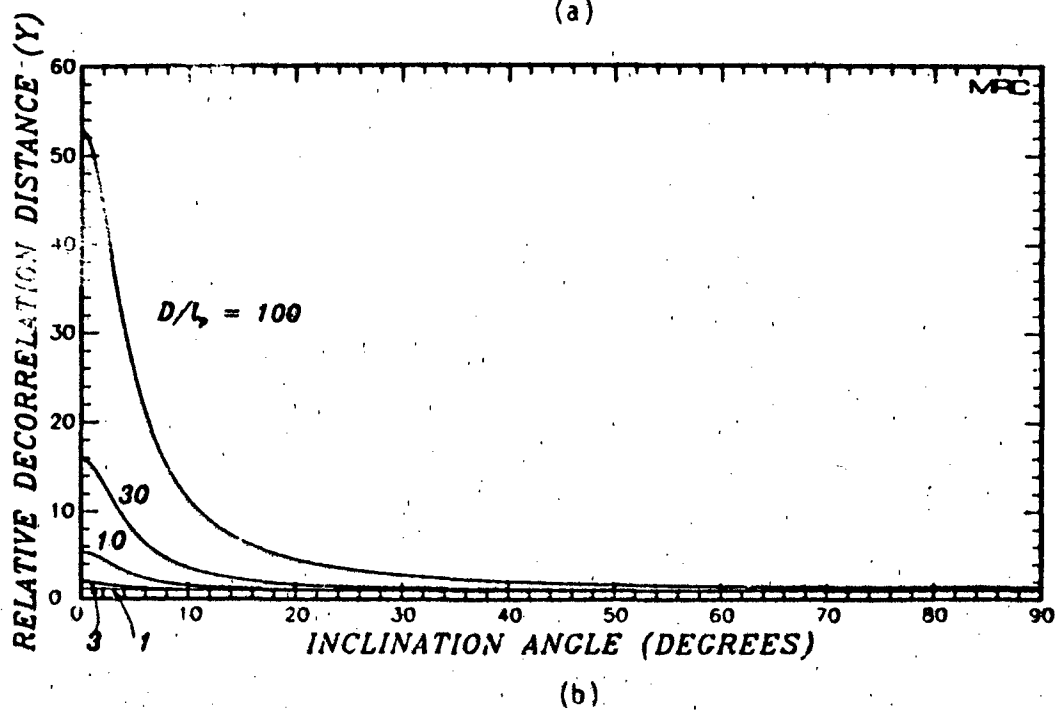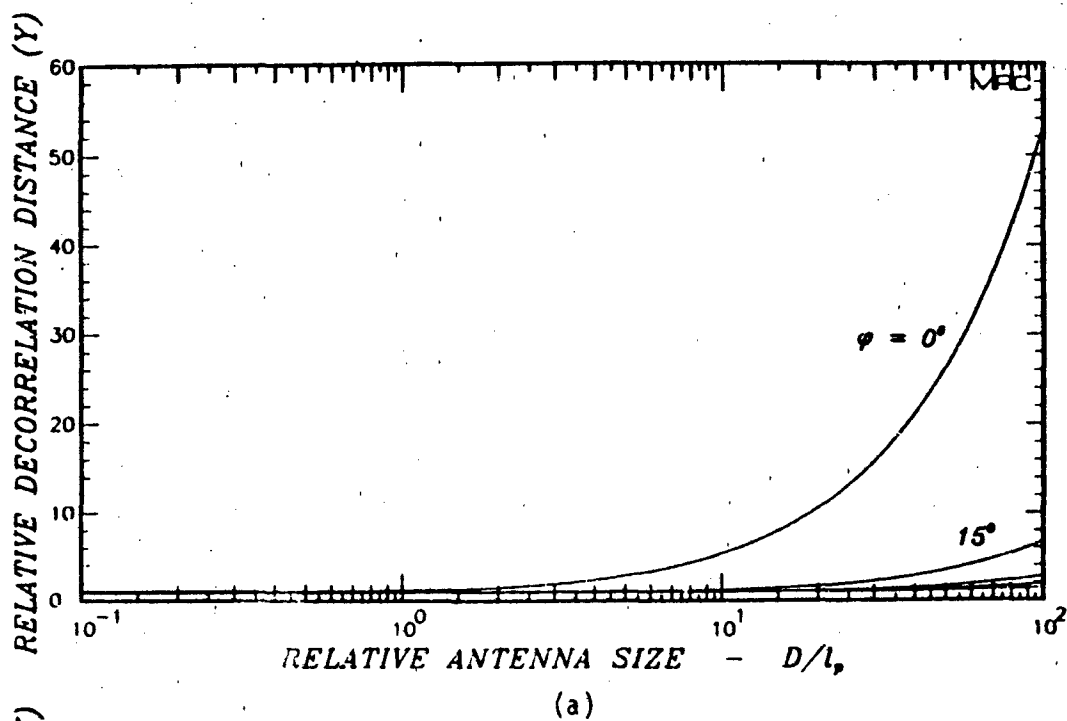40

Figure 8.   Relative signal decorrelation distance in the y-direction
for monostatic radar; a) versus relative antenna size; b)
versus inclination angle.

Mean Time Delay and Time Delay Jitter

In the same manner that an aperture antenna with a small beam-width neglects or averages out energy incident at off-boresight angles to reduce the received power, it also acts to reduce the measured time delay and time delay jitter. This reduction occurs because the energy arriving from directions away from boresight typically travels over longer paths than the more direct signal. These longer paths require a longer propagation time for that portion of the received signal and hence contribute to increased $\langle \tau \rangle$ and σ_τ values. If this energy is neglected by an aperture antenna, then the signal at the output will be characterized by smaller $\langle \tau \rangle$ and σ_τ than that measured by an omnidirectional (point) antenna.

Now define the mean time delay, $\langle \tau \rangle$, as

$$\langle \tau \rangle = \frac{\int G(0,\tau)\tau \, d\tau}{\int G(0,\tau)d\tau} \tag{62}$$

and define the time delay jitter, σ_τ, by the second moment

$$\sigma_\tau^2 = \frac{\int G(0,\tau)\tau^2 d\tau}{\int G(0,\tau)d\tau} - \langle \tau \rangle^2 \tag{63}$$

where $G(0,\tau)$ is the power impulse response measured at the output of the receiving antenna due to an impulse of power originating from the transmitter.

To compute $\langle \tau \rangle$ and σ_τ for the one-way propagation path with transmit and receive aperture antennas, it is convenient to utilize Equation 46 for the power impulse response function. The integrals of τ and τ^2 give first and second derivatives of delta functions which yield first and second derivatives of $\hat{r}_{tr}(\overline{K},\omega_d)$. These derivatives are evaluated at zero ω_d as a result of the τ integration. The remaining integration with respect to $\overline{K}$ is easily performed. The results may be written as

$$\langle \tau \rangle = \frac{1}{2\omega'} \left[\left(1 + \frac{2\sigma_{\theta x}^2}{\theta_r^2} + \frac{2\sigma_{\theta x'}^2}{\theta_t^2} \right)^{-1} \right.$$

$$\left. + \Delta^2 \left(1 + \frac{2\sigma_{\theta y}^2}{\theta_r^2} + \frac{2\sigma_{\theta y'}^2}{\theta_t^2} \right)^{-1} \right] \qquad (64)$$

$$\sigma_\tau^2 = \frac{\sigma_\phi^2}{\omega_0^2} + \frac{1}{2\omega'^2} \left[\left(1 + \frac{2\sigma_{\theta x}^2}{\theta_r^2} + \frac{2\sigma_{\theta x'}^2}{\theta_t^2} \right)^{-2} \right.$$

$$\left. + \Delta^4 \left(1 + \frac{2\sigma_{\theta y}^2}{\theta_r^2} + \frac{2\sigma_{\theta y'}^2}{\theta_t^2} \right)^{-2} \right] \qquad (65)$$

Figure 9 shows the effect of aperture antennas on the observed mean time delay by showing the mean time delay normalized by the value observed with omnidirectional antennas, $(1+\Delta^2)/(2\omega')$. In the figure, transmit and receive apertures are identical and the equivalent phase-screen is assumed to be located midway between the antennas. Figure 9(a) shows the relative mean time delay as a function of D/ℓ_p for values of the inclination angle of 0°, 15°, 30°, 45° and 90°. It is seen that large apertures can have a significant effect in reducing the observed mean time delay, particularly when the direction of propagation is close to the magnetic field direction. In Figure 9(b) the abscissa and the parametric quantity are interchanged relative to Figure 9(a).

Figures 10(a-b) show the effect of aperture antennas on the observed time delay jitter σ_τ. Here σ_τ is normalized to its value for omnidirectional transmit and receive antennas $[(1+\Delta^4)/(2\omega'^2)]^{1/2}$. It is further assumed that the ratio σ_ϕ/ω_0 is small, as is always the case for GHz and higher frequencies. At $\psi = 0°$ the antenna aperture has identical effects on σ_τ and $\langle \tau \rangle$. At other values of the inclination

43
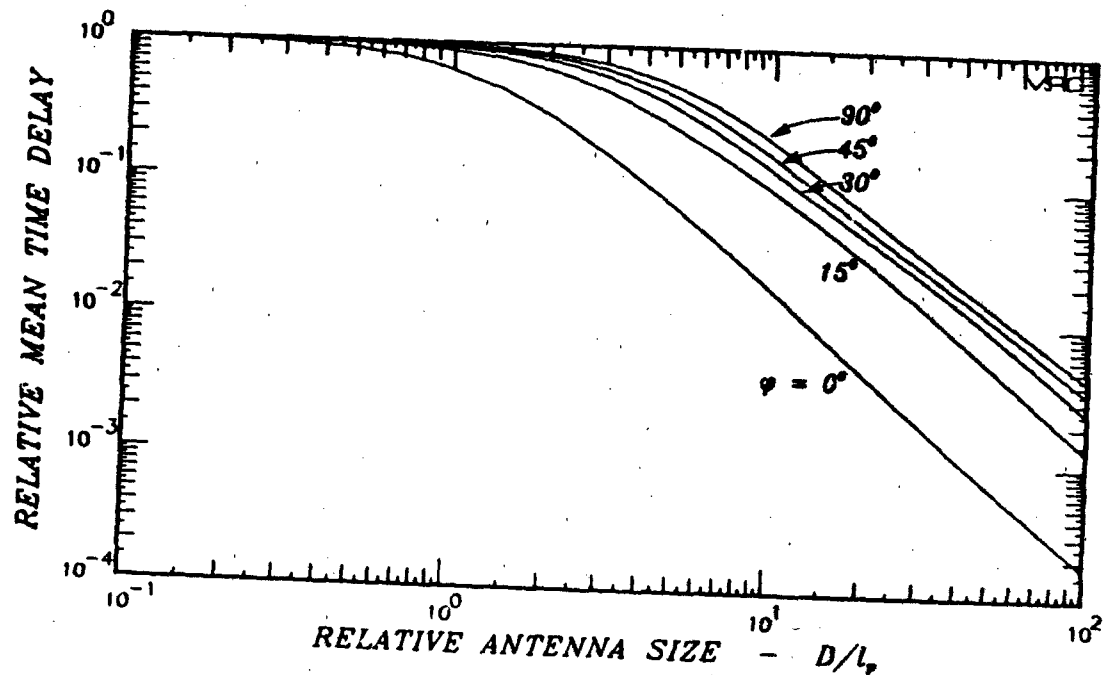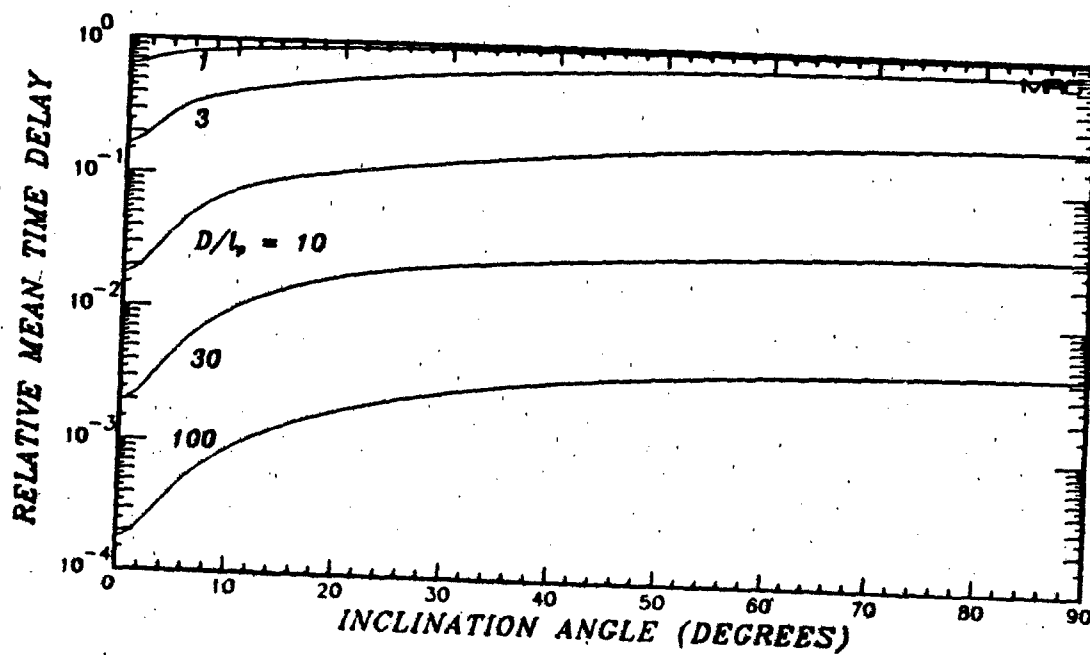
Figure 9. Relative mean time delay for one-way path with transmit and receive aperture antennas; a) versus relative antenna size; b) versus inclination angle.
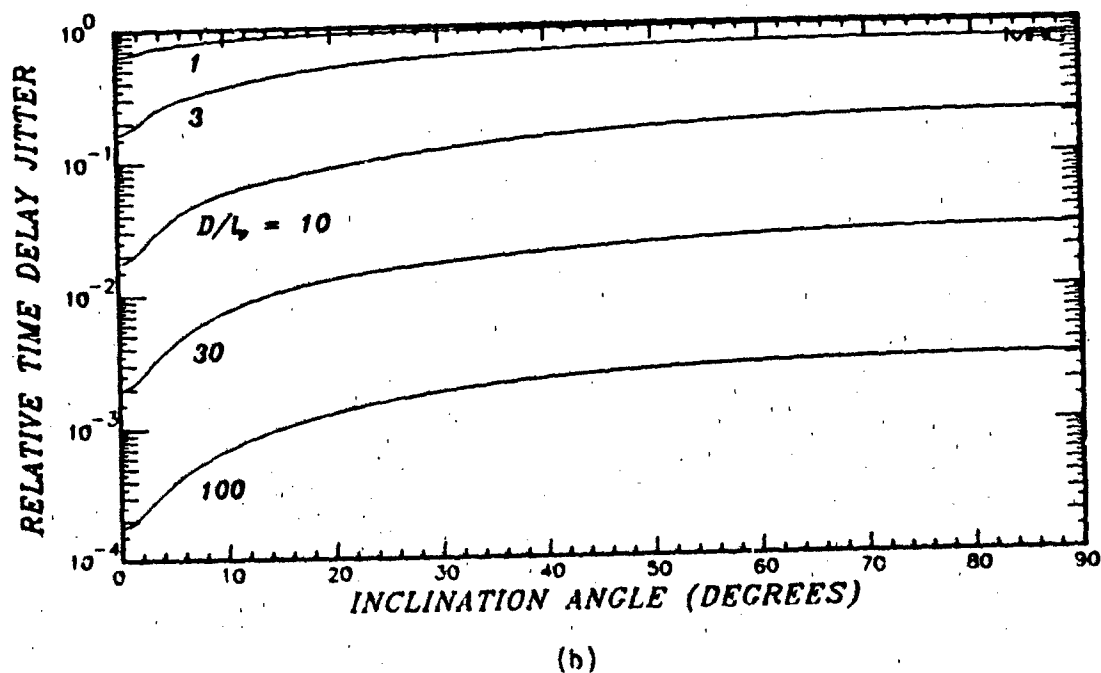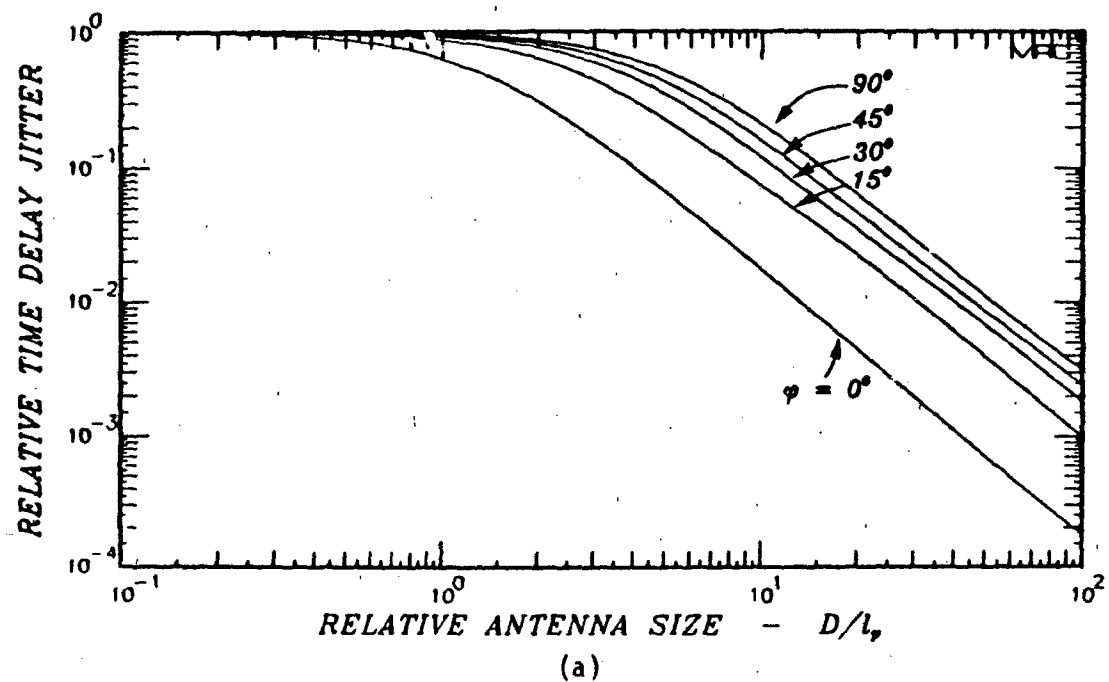
Figure 10. Relative time delay jitter for one-way path with transmit and receive aperture antennas; a) versus relative antenna size; b) versus inclination angle.

angle ψ, the results shown in Figure 10 are similar but not identical to those shown in Figure 9. The decreased measurements of $<\tau>$ and σ_τ are the result of the action of the antenna to exclude signal energy incident from off-axis directions that arrives later than energy that propagates over the direct path.

For the general case that the power impulse response function is given as the convolution of two other functions as by Equation 52, it is easy to perform the required τ integrations to obtain

$$<\tau_m> = <\tau_1> + <\tau_2> \tag{66}$$

$$\sigma^2_{\tau m} = \sigma^2_{\tau 1} + \sigma^2_{\tau 2} \tag{67}$$

These results state that the mean time delay and time delay variance are the sums of the values obtained over each of the two one-way propagation paths. The required one-way values may be obtained from Equations 64-65 with attention to the direction of propagation and antenna placement. The final results are

$$<\tau> = \frac{1}{\omega'}\left[\left(1 + \frac{2\sigma^2_{\theta x'}}{\theta_t^2}\right) + \Delta^2\left(1 + \frac{2\sigma^2_{\theta y'}}{\theta_t^2}\right)\right]^{-1} \tag{68}$$

$$\sigma^2_\tau = \frac{2\sigma^2_\phi}{\omega_0^2} + \frac{1}{\omega'^2}\left[\left(1 + \frac{2\sigma^2_{\theta x'}}{\theta_t^2}\right)^{-2} + \Delta^4\left(1 + \frac{2\sigma^2_{\theta y'}}{\theta_t^2}\right)^{-2}\right] \tag{69}$$

Figures 11-12 show the values of mean time delay and time delay jitter for an aperture antenna normalized to their values for an omni-directional antenna. Again the factor σ_ϕ/ω_0 is assumed small for this monostatic radar case. These normalized results are very similar in form to those presented in Figures 9-10 and again show the dramatic effect of a large aperture antenna that operates in strong scattering conditions.

Coherence Bandwidth

The coherence bandwidth is appropriately chosen as the inverse of the time delay jitter exhibited by the received waveform due to a transmitted power that is a delta function in delay (Knepp, 1983(b)). In the cases considered here where σ_ϕ/ω_0 is small, the effects of antenna apertures on the measured coherence bandwidth are easily obtained from Equations 65 and 69. The results for the one-way propagation path with transmit and receive antennas and for the monostatic radar case are given as the reciprocal of the values shown in Figures 10 and 12, respectively.
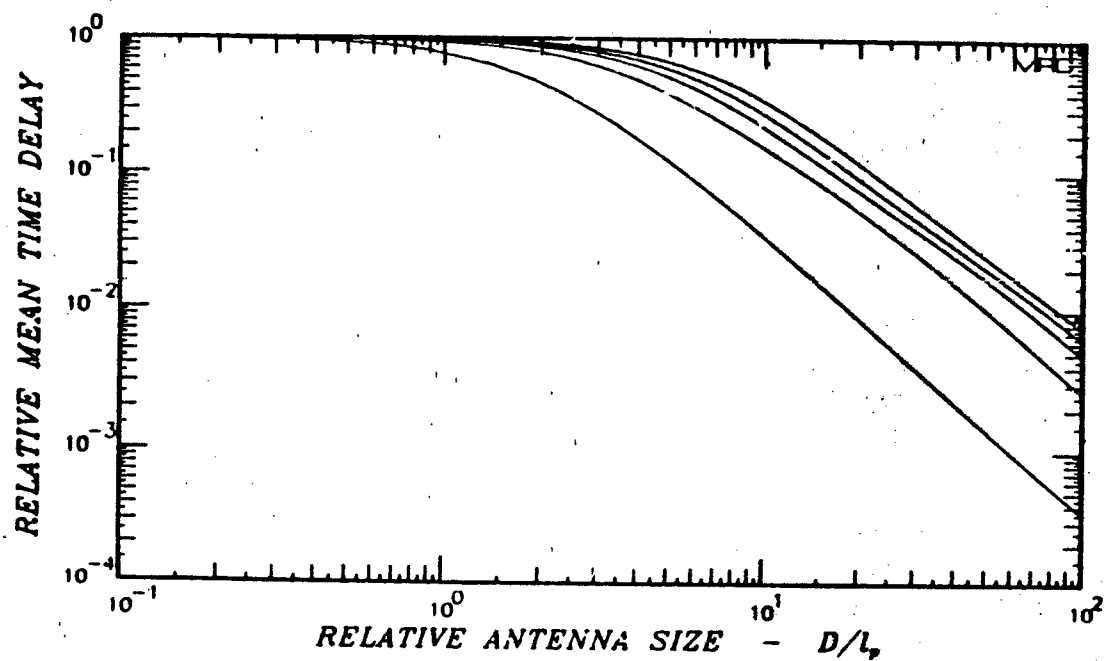
(a)
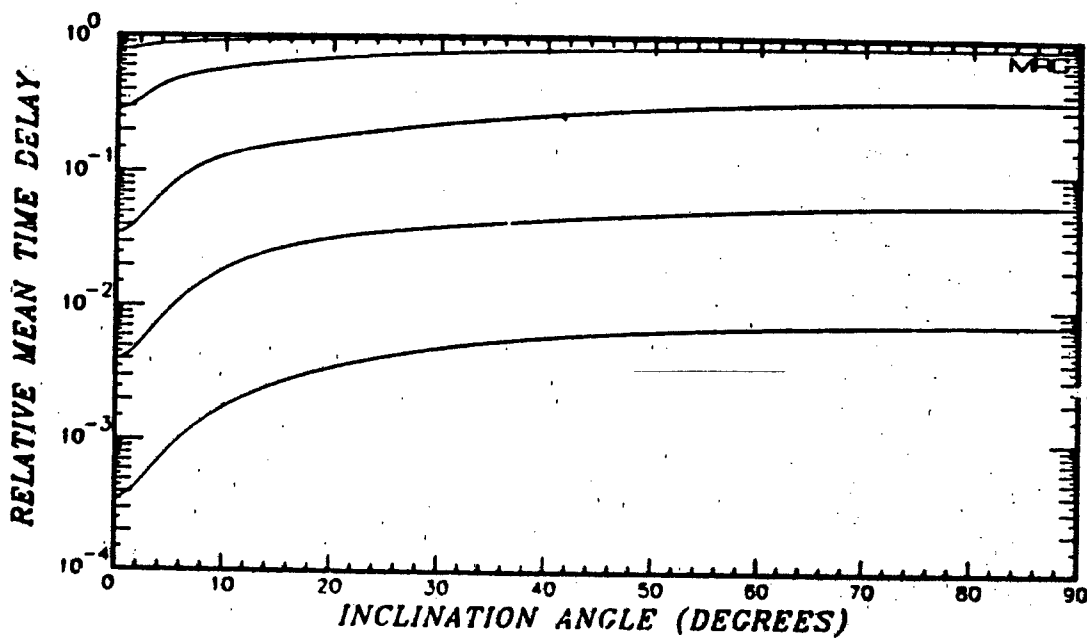
(b)

Figure 11.   Relative mean time delay for monostatic radar; a) versus relative antenna size; b) versus inclination angle.

48

(a)

(b)
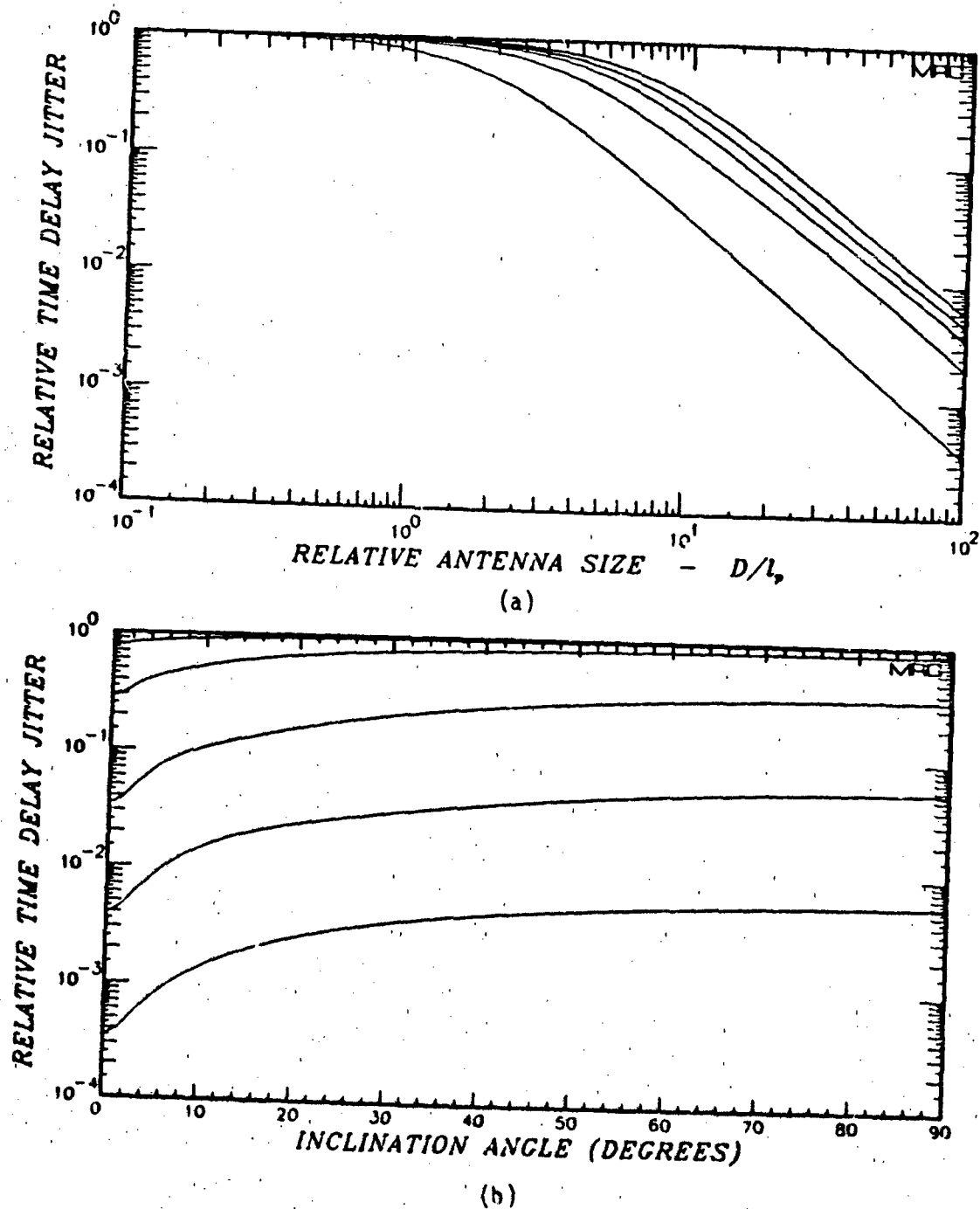
Figure 12.   Relative time delay jitter for monostatic radar; a) versus
relative antenna size; b) versus inclination angle.

49

REFERENCES

Arendt, P. R., and H. Soicher, "Effects of Arctic Nuclear Explosions on Satellite Radio Communication," Proc. IEEE, Vol. 52, No. 6, pp. 672-676, June 1964.

Briggs, B. H., and I. A. Parkin, "On the Variation of Radio Star and Satellite Scintillations with Zenith Angle," J. Atmos. Terr. Phys., Vol. 25, pp. 339-365, 1963.

Davis, T. N., G. J. Romick, E. M. Westcott, R. A. Jeffries, D. M. Kerr, and H. M. Peek, "Observations of the Development of Striations in Large Barium Clouds," Planet. Space Science, Vol. 22, p. 67, 1974.

Fante, R. L., "Two-position, Two-frequency Mutual-coherence Function in Turbulence," J. Opt. Soc. Am., Vol. 71, No. 12, pp. 1446-1451, December 1981.

Fante, R. L., "Electromagnetic Beam Propagation in Turbulent Media," Proc. IEEE, Vol. 63, No. 12, pp. 1669-1692, December 1975.

Fante, R. L., "Some Physical Insights into Beam Propagation in Strong Turbulence," Radio Science, Vol. 15, No. 4, pp. 757-762, July-August 1980.

Fremouw, E. J., R. L. Leadabrand, R. C. Livingston, M. D. Cousins, C. L. Rino, B. C. Fair and R. A. Long, "Early Results from the DNA Wideband Satellite Experiment-Complex Signal Scintillation," Radio Science, Vol. 13, No. 1, pp. 167-187, January-February 1978.

Fried, D. L., "Aperture Averaging of Scintillation," J. Opt. Soc. Amer., Vol. 57, pp. 169-180, February 1967.

Homstad, G. E., J. W. Strohbehn, R. H. Berger, and J. M. Henegan, "Aperture Averaging Effects for Weak Scintillations," J. Opt. Soc. Amer., Vol. 64, pp. 162-165, February 1974.

Ishimaru, A., Wave Propagation and Scattering in Random Media, New York: Academic Press, 1978.

Ishimaru, A., "Fluctuations of a Beam Wave Propagating Through A Locally Homogeneous Medium," Radio Science, Vol. 4, pp. 295-305, April 1969.

REFERENCES (Continued)

King, M. A., and P. B. Fleming, "An Overview of the Effects of Nuclear Weapons on Communications Capabilities," Signal, pp. 59-66, January 1980.

Knepp, D. L., "Antenna Aperture Effects on Measurements of Propagation Through Turbulence," IEEE Trans. Antennas Propagat., Vol. AP-23, pp. 682-687, September 1975.

Knepp, D. L., Multiple Phase-Screen Propagation Analysis for Defense Satellite Communications System, DNA 4424T, MRC-R-332, Mission Research Corporation, September 1977.

Knepp, D. L., The Effects of Aperture Antennas After Signal Propagation Through Anisotropic Ionized Media, Contract DNA 001-81-C-0006, MRC-R-744, Mission Research Corporation, March 1983(a).

Knepp, D. L., "Analytic Solution for the Two-Frequency Mutual Coherence Function for Spherical Wave Propagation," Radio Science, Vol. 18, No. 4, pp. 535-549, July-August 1983(b).

Knepp, D. L., and L. A. Wittwer, "Simulation of Wide Bandwidth Signals That Have Propagated Through Random Media," Radio Science, (in press), January-February 1984.

Lee, R. W., and J. C. Harp, "Weak Scattering in Random Media, with Applications to Remote Probing," Proc. IEEE, Vol. 57, pp. 375-406, April 1969.

Papoulis, A., Probability, Random Variables, and Stochastic Processes, McGraw Hill: New York, 1965.

Pope, J. H., and R. B. Fritz, "High Latitude Scintillation Effects on Very High Frequency (VHF) and S-band Satellite Transmissions," Indian J. Pure App. Phys., Vol. 9, pp. 593-600, August 1971.

Price, G. H., W. G. Chesnut, and A. Burns, Monopulse Radar Propagation Through Thick, Structured Ionziation, Special Report 4, Contract DASA01-69-C-0126, SRI Project 8047, Stanford Research Institute, April 1972.

Salpeter, E. E., "Interplanetary Scintillations. I. Theory," Astrophys. J., Vol. 147, pp. 433-448, 1967.

REFERENCES (Concluded)

Skinner, N. J., R. F. Kelleher, J. B. Hacking and C. W. Benson, "Scintillation Fading of Signals in the SHF Band," Nature (Phys. Sci.), Vol. 232, pp. 19-21, 5 July 1971.

Sreenivasiah, I., and A. Ishimaru, "Beam Wave Two-frequency Mutual-coherence Function and Pulse Propagation in Random Media: An Analytic Solution," Applied Optics, Vol. 18, No. 10, pp. 1613-1618, May 1979.

Sreenivasiah, I., A. Ishimaru, and S. T. Hong, "Two-frequency Mutual Coherence Function and Pulse Propagation in a Random Medium: An Analytic Solution to the Plane Wave Case," Radio Science, Vol. 11, No. 10, pp. 775-778, October 1976.

Tatarskii, V. I., The Effects of the Turbulent Atmosphere on Wave Propagation, translated by Israel Program for Scientific Translations, National Technical Information Service, U.S. Department of Commerce, 1971.

Taur, R. R., "Simultaneous 1.5- and 4-GHz Ionospheric Scintillation Measurements," Radio Science, Vol. 11, pp. 1029-1036, December 1976.

Wandzura, S. A., "Meaning of Quadratic Structure Functions," J. Opt. Soc. Am., Vol. 70, No. 6, pp. 745-747, June 1980.

Wheelon, A. D., "Relation of Radio Measurements to the Spectrum of Tropospheric Dielectric Fluctuations," J. Appl. Phys., vol. 28, pp. 684-693, June 1957.

Wheelon, A. D., "Radio-Wave Scattering by Tropospheric Irregularities," J. Res. Nat. Bur. Stand., Vol. 63D, pp. 205-233, September 1959.

Wittwer, L. A., Radio Wave Propagation in Structured Ionization for Satellite Applications, DNA 5304D, Defense Nuclear Agency, December 1979.

Wolcott, J. H., D. J. Simons, T. E. Eastman, and T. J. Fitzgerald, "Characteristics of Late-Time Striations Observed During Operation STRESS," Effect of the Ionosphere on Space and Terrestrial Systems, edited by J. M. Goodman, pp. 602-613, U.S. Government Printing Office, 1978.

Yeh, K. C., and C. H. Liu, "An Investigation of Temporal Moments of Stochastic Waves," Radio Science, Vol. 12, No. 5, pp. 671-680, September-October 1977.

APPENDIX

IONIZATION IRREGULARITY DESCRIPTION

The ionization irregularities are assumed to be elongated along the direction of the earth's magnetic field as shown in Figure A-1. The electromagnetic wave propagates in the negative z direction. The magnetic field vector lies in the y-z plane at an angle of ψ with respect to the z axis. The ionization irregularities are assumed rotationally symmetric with autocorrelation function

$$B_\xi(r,s) = \frac{\sigma_{N_e}^2}{\langle N_e \rangle^2} \exp\left\{ - \frac{r^2}{r_0^2} - \frac{s^2}{(qr_0)^2} \right\} \qquad (A-1)$$
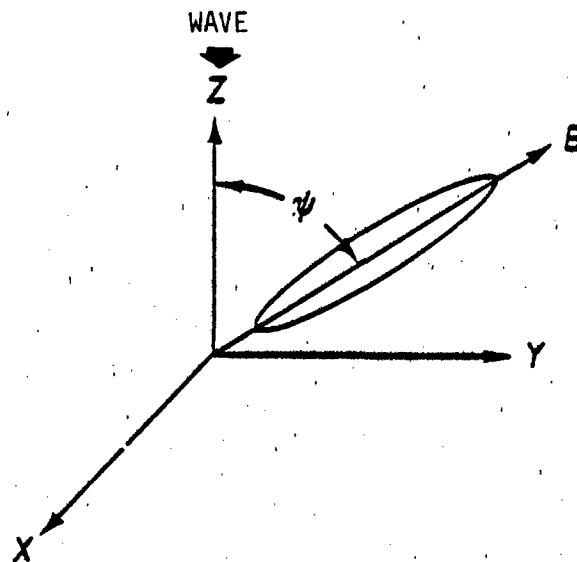
Figure A-1. A single irregularity elongated along the magnetic field line in the y-z plane.

where s is measured along the magnetic field direction and r is measured perpendicular to this direction. The quantity q is known as the axial ratio (Briggs and Parkin, 1963) and r_0 is the correlation distance or irregularity scale size.

The s, r coordinate system may be related to the x, y, z system by the equations $s^2 = (y \sin \psi + z \cos \psi)^2$ and $r^2 = x^2 + (y \cos \psi - z \sin \psi)^2$. Using the above transformation the irregularity correlation function may be expressed in the x, y, z. This expression can easily be integrated according to Equation 6 to obtain the function $A(\zeta, n)$ as

$$A(\zeta, n) = \frac{\sigma_{N_e}^2 \sqrt{\pi} \, qr_0}{<N_e>^2 (q^2 \sin^2 \psi + \cos^2 \psi)^{1/2}}$$

$$\times \exp \left\{ - \frac{\zeta^2}{r_0^2} - \frac{n^2}{r_0^2 (q^2 \sin^2 \psi + \cos^2 \psi)} \right\} \qquad (A-2)$$

The above equation is essentially Equation 10 in Briggs and Parkin (1963). $A(\zeta, n)$ is easily expanded in a Taylor series and, retaining only terms up to the quadratic, one obtains Equation 10 in the text where

$$A_0 = \frac{\sigma_{N_e}^2 \sqrt{\pi} \, qr_0 \Delta}{<N_e>^2} \qquad (A-3)$$

$$A_2 = \frac{- \sigma_{N_e}^2 \sqrt{\pi} \, q\Delta}{<N_e>^2 r_0} \qquad (A-4)$$

$$\Delta^2 = \frac{1}{q^2\sin^2\psi + \cos^2\psi} \qquad (A-5)$$

This same formalism may also be applied to irregularity power spectra that are non-Gaussian. For the case of a power-law PSD the coefficients A_0 and A_2 are different than above but behave in essentially the same manner as a function of the outer scale size as long as the three-dimensional in-situ electron density PSD falls off at least as rapidly as K^{-4}.

Phase Standard Deviation

For an ionized medium, the phase standard deviation is given as the integral of the irregularity autocorrelation function along the direction of propagation (Salpeter, 1967). The result may be written as (Knepp, 1983(b))

$$\sigma_\phi^2 = \frac{1}{4} k_p^4 L A_0 / k_0^2 \qquad (A-6a)$$

or

$$\sigma_\phi^2 = \sqrt{\pi} \ (\lambda r_e)^2 q \Delta r_0 L \sigma_{N_e}^2 \qquad (A-6b)$$

Theoretical Angle-Of-Arrival Fluctuation

Consider a plane wave traveling in the negative z-direction and incident in the x-y plane at an angle θ from the z-axis. The electric field is given by $E(x,y) = E_0 \exp\{ik(\sin\theta \ x + \cos\theta \ z)\}$ where the $\exp(i\omega t)$ time dependence is suppressed. The angle-of-arrival measured along the x-axis is computed as

$$\theta_x = \frac{1}{ikE_o} \frac{\partial E(x,z)}{\partial x} \tag{A-7}$$

This computation gives $\sin \theta$ which, in the small angle limit, is approximately θ.

In the case of interest here the incident field is given as the solution to the parabolic wave equation and the angle-of-arrival may be measured in the x-direction as

$$\theta_x = \frac{1}{ikU_o} \frac{\partial U(\overline{\rho},z,\omega)}{\partial x} \tag{A-8}$$

with a similar expression for θ_y. Here the measurement depends on the frequency. At a single frequency the rms value of θ_x is related to the second derivative of the two-position MCF (Papoulis, 1965, p. 317)

$$\sigma_{\theta x}^2 = -\frac{1}{k^2} \left. \frac{\partial^2 \Gamma(\zeta,\eta,\omega_d=0)}{\partial \zeta^2} \right|_{\zeta=\eta=0} \tag{A-9}$$

With a similar equation for $\sigma_{\theta y}$. For the case of propagation from a transmitter in the $-z_t$ plane to a receiver in the z_r plane, $\sigma_{\theta x}$ and $\sigma_{\theta y}$ may be obtained from derivatives of Equation 25 in the text as $\sigma_{\theta x} = \sqrt{2}/(k \ell_o)$ and $\sigma_{\theta y} = \sqrt{2}/[k(\ell_o/\Delta)]$.

For the case of propagation from a transmitter in the z_r plane to a receiver in the $-z_t$ plane, the interchange of transmitter and receiver may be taken into account by substituting ℓ_o' for ℓ_o where $\ell_o' = z_t \ell_o / z_r$. This substitution gives the angle-of-arrival fluctuation over the reversed path as $\sigma_{\theta x'} = \sqrt{2}/(k \ell_o')$ and $\sigma_{\theta y'} = \sqrt{2}/[k(\ell_o'/\Delta)]$.

56

DISTRIBUTION LIST

DEPARTMENT OF DEFENSE

Asst to the Sec of Def, Atomic Energy
    ATTN: Exec Asst

Defense Advanced Rsch Proj Agency
    ATTN: GSD, R. Alewine
    ATTN: STO, N. Doherty
    ATTN: STO, W. Kurowski

Defense Comm Agency
    ATTN: Code 205
    ATTN: Code 230
    ATTN: J300 for Yen-Sun Fu

Defense Comm Engr Ctr
    ATTN: Code R123, Tech Lib
    ATTN: Code R410
    ATTN: Code R410, N. Jones

Defense Intell Agency
    ATTN: DB, A. Wise
    ATTN: DB-4C
    ATTN: DC-7B
    ATTN: Dir
    ATTN: DT-1B

Defense Nuclear Agency
    ATTN: NATF
    ATTN: NAWE
    ATTN: RAAE, P. Lunn
    ATTN: RAAE, K. Schwartz
    ATTN: RAEE
    ATTN: STNA
3 cys ATTN: RAAE
4 cys ATTN: STTI-CA

Defense Tech Info Center
12 cys ATTN: DD

Dep Under Sec of Def, Comm, Cmd, Cont & Intell
    ATTN: Dir of Intell Sys

Field Command, DNA, Det 1
Lawrence Livermore National Lab
    ATTN: FC-1

Field Command, Defense Nuclear Agency
    ATTN: FCPR
    ATTN: FCTT, W. Summa
    ATTN: FCTXE

Interservice Nuc Wpns School
    ATTN: TTV

Joint Chiefs of Staff
    ATTN: C3S
    ATTN: C3S, Eval Ofc. (HDOO)

Joint Data System Support Ctr
    ATTN: C-312, R. Mason
    ATTN: C-500
    ATTN: G510, G. Jones
    ATTN: G510, P. Bird

Under Sec of Def for Rsch & Engrg
    ATTN: Strat & Space Sys (OS)

DEPARTMENT OF DEFENSE (Continued)

Joint Strat Tgt Planning Staff
    ATTN: JLAA
    ATTN: JLK, DNA Rep
    ATTN: JLKS
    ATTN: JPPFD
    ATTN: JPSS
    ATTN: JPTM

National Security Agency
    ATTN: B-43, C. Goedeke
    ATTN: W-36, O. Bartlett

WWMCCS Sys Engrg Org
    ATTN: R. Crawford

DEPARTMENT OF THE ARMY

Army Logistics Management Ctr
    ATTN: DLSIE

Asst Ch of Staff for Automation & Comm
    ATTN: DAMO-C4, P. Kenny

US Army Electronics R&D Command
    ATTN: DELAS-EO, F. Niles

BMD Advanced Tech Ctr
    ATTN: ATC-O, W. Davies
    ATTN: ATC-R, D. Russ
    ATTN: ATC-R, W. Dickinson
    ATTN: ATC-T, M. Capps

BMD Systems Command
    ATTN: BMDSC-LEE, R. Webb
2 cys ATTN: BMDSC-HW

Dep Ch of Staff ofr Ops & Plans
    ATTN: DAMO-RQC, C2 Div

Harry Diamond Laboratories
    ATTN: DELHD-NW-R, R. Williams, 22000
2 cys ATTN: DELHD-NW-P, 20240

US Army Chem School
    ATTN: ATZN-CM-CS

US Army Comm-Elec Engrg Instal Agency
    ATTN: CC-CE-TP, W. Nair

US Army Comm Command
    ATTN: CC-OPS-W
    ATTN: CC-OPS-WR, H. Wilson

US Army Comm R&D Command
    ATTN: DRDCO-COM-RY, W. Kesselman

US Army Foreign Science & Tech Ctr
    ATTN: DRXST-SD

US Army Material Command
    ATTN: DRCLDC, J. Bender

US Army Nuc & Chem Agency
    ATTN: Library

DEPARTMENT OF THE ARMY (Continued)

US Army Satellite Comm Agency
        ATTN: Doc Control

US Army TRADOC Sys Analysis Actvy
        ATTN: ATAA-PL
        ATTN: ATAA-TCC, F. Payan, Jr
        ATTN: ATAA-TDC

US Army White Sands Missile Range
        ATTN: STEWS-TE-N, K. Cummings

USA Missile Command
        ATTN: DPSMI-YSO, J. Gamble

DEPARTMENT OF THE NAVY

Joint Cruise Missiles Proj Ofc
        ATTN: JCMG-707

Naval Air Systems Command
        ATTN: PMA 271

Naval Electronic Systems Command
        ATTN: Code 3101, T. Hughes
        ATTN: Code 501A
        ATTN: PME 106-4, S. Kearney
        ATTN: PME 117-20
        ATTN: PME 117-211, B. Kruger
        ATTN: PME-106, F. Diederich
        ATTN: PME-117-2013, G. Burnhart

Naval Intell Support Ctr
        ATTN: NISC-50

Naval Ocean Systems Center
        ATTN: Code 532
        ATTN: Code 5322, M. Paulson
        ATTN: Code 5323, J. Ferguson

Naval Research Laboratory
        ATTN: Code 4187
        ATTN: Code 4700
        ATTN: Code 4700, S. Ossakow
        ATTN: Code 4720, J. Davis
        ATTN: Code 4780
        ATTN: Code 6700
        ATTN: Code 7500, B. Wald
        ATTN: Code 7950, J. Goodman

Naval Space Surveillance System
        ATTN: J. Burton

Naval Surface Wpns Ctr
        ATTN: Code F31

Naval Telecommunications Command
        ATTN: Code 341

Ofc of the Dep Ch of Naval Ops
        ATTN: NOP 654, Strat Eval & Anal Br
        ATTN: NOP 941D
        ATTN: NOP 981N

Ofc of Naval Rsch
        ATTN: Code 412, W. Condell

Theater Nuc Warf Proj Ofc
        ATTN: PM-23, D. Smith

DEPARTMENT OF THE NAVY (Continued)

Strategic Systems Project Ofc
        ATTN: NSP-2141
        ATTN: NSP-2722
        ATTN: NSP-43, Tech Lib

DEPARTMENT OF THE AIR FORCE

Air Force Geophysics Laboratory
        ATTN: CA, A. Stair
        ATTN: LIS, J. Buchau
        ATTN: LYD, K. Champion
        ATTN: OPR, H. Gardiner
        ATTN: OPR-1
        ATTN: R. Babcock
        ATTN: R. O'Neil

Air Force Operational Test & Eval Ctr
        ATTN: OAS
        ATTN: TES

Air Force Satellite Ctrl Facility
        ATTN: WE

Air Force Space Technology Ctr
        ATTN: YH

Air Force Tech Appl Ctr
        ATTN: TN

Air Force Wpns Laboratory
        ATTN: NTN
        ATTN: NTY
        ATTN: SUL

Air Force Wright Aeronautical Lab/AAAD
        ATTN: A. Johnson
        ATTN: W. Hunt

Air Logisitcs Command
        ATTN: OO-ALC/MM

Air University Library
        ATTN: AUL-LSE

Asst Ch of Staff, Studies & Analysis
        ATTN: AF/SASC, C. Rightmeyer

Ballistic Missile Ofc/DAA
        ATTN: ENSN
        ATTN: ENSN, W. Wilson
        ATTN: SYC, D. Kwan

Dep Ch of Staff, Rsch, Dev & Acq
        ATTN: AFRDQI
        ATTN: AFRDS, Space Sys & C3 Dir

Dep Ch of Staff, Plans & Opns
        ATTN: AFXOKCD
        ATTN: AFXOKS
        ATTN: AFXOKT

Electronic Systems Div
        ATTN: SCS-1E
        ATTN: SCS-2. G. Vinkels

Foreign Tech Div
        ATTN: NIIS, Library
        ATTN: TQTD, B. Ballard

DEPARTMENT OF THE AIR FORCE (Continued)

Rome Air Development Center
    ATTN: OCS, V. Coyne
    ATTN: OCSA, R. Schneible
    ATTN: TSLD

Rome Air Development Ctr
    ATTN: EEP, J. Rasmussen
    ATTN: EEPS, P. Kossey

Space Command
    ATTN: DC, T. Long
    ATTN: XPSD

Space Division, Worldway Postal Center
    ATTN: YC
    ATTN: YG
    ATTN: YK
    ATTN: YNC

Strategic Air Command
    ATTN: ADWA
    ATTN: DCX
    ATTN: DCZ
    ATTN: NRI/STINFO Library
    ATTN: XPF, B. Stephan
    ATTN: XPFC
    ATTN: XPFS
    ATTN: XPQ

DEPARTMENT OF ENERGY

Department of Energy, GTN
    ATTN: DP-233

OTHER GOVERNMENT AGENCIES

Bureau of Politico Mil Affairs
    ATTN: PM/STM

Central Intell Agency
    ATTN: OSWR/NED
    ATTN: OSWR/SSD for K. Feuerpfetl

National Bureau of Standards
    ATTN: Sec Ofc for R. Moore

National Oceanic & Atomospheric Admin
    ATTN: R. Grubb

Institute for Telecommunications Sci
    ATTN: A. Jean
    ATTN: E. Morrison
    ATTN: L. Berry
    ATTN: W. Utlaut

NASA
    ATTN: R. Jost

NATO

NATO School, SHAPE
    ATTN: US Documents Officer

DEPARTMENT OF ENERGY CONTRACTORS

University of California
Lawrence Livermore National Lab
    ATTN: L-31, R. Hager
    ATTN: Tech Info Dept Library

DEPARTMENT OF ENERGY CONTRACTORS (Continued)

Los Alamos National Laboratory
    ATTN: D. Sappenfield
    ATTN: D. Simons
    ATTN: G-6, E. Jones
    ATTN: J. Hopkins
    ATTN: J. Wolcott
    ATTN: MS 664, J. Zinn
    ATTN: P. Keaton
    ATTN: R. Jeffries
    ATTN: T. Kunkle, ESS-5

Sandia National Laboratories
    ATTN: B. Murphey
    ATTN: R. Grossman
    ATTN: T. Cook

Sandia National Laboratories
    ATTN: D. Dahlgren
    ATTN: D. Thornebrough
    ATTN: Org 1231, P. Backstrom
    ATTN: Org 1250, W. Brown
    ATTN: Org 4231, T. Wright
    ATTN: Space Project Div
    ATTN: Tech Lib, 3141

EG&G, Inc
Attention Doc Control for
    ATTN: D. Wright
    ATTN: J. Colvin

DEPARTMENT OF DEFENSE CONTRACTORS

Aerospace Corp
    ATTN: D. Olsen
    ATTN: D. Whelan
    ATTN: E. Rodriguez
    ATTN: F. Djuth
    ATTN: I. Garfunkel
    ATTN: J. Kluck
    ATTN: J. Straus
    ATTN: K. Cho
    ATTN: R. Slaughter
    ATTN: T. Salmi
    ATTN: V. Josephson

Aerospace Corp
    ATTN: S. Mewaters

Analytical Systems Engrg Corp
    ATTN: Radio Sciences

Analytical Systems Engrg Corp
    ATTN: Security

Austin Research Assoc
    ATTN: B. Moore
    ATTN: J. Thompson
    ATTN: J. Uglum
    ATTN: M. Sloan

BDM Corp
    ATTN: L. Jacobs
    ATTN: T. Neighbors

Berkeley Rsch Assoc, Inc
    ATTN: C. Prettie
    ATTN: J. Workman
    ATTN: S. Brecht

DEPARTMENT OF DEFENSE CONTRACTORS (Continued)

Boeing Co
      ATTN: G. Hall

Boeing Co
      ATTN: MS 8K-85, Dr. S. Tashird
      ATTN: MS/87-63, D. Clauson

BR Communications
      ATTN: J. McLaughlin

Univ of California
      ATTN: H. Booker

California Institute of Technology
      ATTN: C. Elachi

California Rsch & Tech, Inc
      ATTN: M. Rosenblatt

Charles Stark Draper Lab, Inc
      ATTN: A. Tetewski
      ATTN: D. Cox
      ATTN: J. Gilmore

Communications Satellite Corp
      ATTN: D. Fang
      ATTN: G. Hyde

Computer Sciences Corp
      ATTN: F. Eisenbarth

Cornell University
      ATTN: D. Farley, Jr
      ATTN: M. Kelly

Electrospace Systems, Inc
      ATTN: H. Logston
      ATTN: P. Phillips

EOS Technologies, Inc
      ATTN: D. Payton

EOS Technologies, Inc
      ATTN: B. Gabbard
      ATTN: W. Lelevier

General Electric Co
      ATTN: A. Steinmayer
      ATTN: C. Zierdt
      ATTN: R. Juner

General Electric Co
      ATTN: G. Millman

General Rsch Corp
      ATTN: B. Bennett

Geo Centers, Inc
      ATTN: E. Marram

GTE Communications Products Corp
      ATTN: A. Murphy
      ATTN: H. Gelman

GTE Govt Systems Corp
      ATTN: R. Steinhoff

Harris Corp
      ATTN: E. Knick

DEPARTMENT OF DEFENSE CONTRACTORS (Continued)

Honeywell, Inc
      ATTN: A. Kearns, MS924-3
      ATTN: G. Terry, Avionics Dept

Horizons Tech, Inc
      ATTN: R. Kruger

HSS, Inc
      ATTN: D. Hansen

IBM Corp
      ATTN: H. Ulander

Institute for Defense Analyses
      ATTN: E. Bauer
      ATTN: H. Gates
      ATTN: H. Wolfhard
      ATTN: J. Aein

ITT Corp
      ATTN: Tech Library

ITT Corp
      ATTN: G. Wetmore

JAYCOR
      ATTN: J. Sperling

JAYCOR
      ATTN: H. Dickinson

Johns Hopkins University
      ATTN: C. Meng
      ATTN: J. Phillips
      ATTN: J. Newland
      ATTN: K. Potocki
      ATTN: R. Stokes, 1-W2S0
      ATTN: T. Evans

Kaman Sciences Corp
      ATTN: E. Conrad

Kaman Tempo
      ATTN: B. Bambill
      ATTN: DASIAC
      ATTN: W. McNamara

Kaman Tempo
      ATTN: DASIAC

Litton Systems, Inc
      ATTN: B. Zimmer

Lockheed Missiles & Space Co, Inc
      ATTN: J. Kumer
      ATTN: R. Sears

Lockheed Missiles & Space Co, Inc
      ATTN: Dept 60-12
   2 cys ATTN: D. Churchill

MIT Lincoln Lab
      ATTN: D. Towle
      ATTN: I. Kupiec
      ATTN: V. Vitto

Magnavox Govt & Indus Electronics Co
      ATTN: G. White

60

DEPARTMENT OF DEFENSE CONTRACTORS (Continued)

M/A Com Linkabit Inc
    ATTN: A. Viterbi
    ATTN: H. Van Trees
    ATTN: I. Jacobs

Maxim Tech, Inc
    ATTN: E. Tsui
    ATTN: J. Marshall
    ATTN: R. Morganstern

McDonnell Douglas Corp
    ATTN: R. Halprin
    ATTN: Tech Lib Services
    ATTN: W. Olson

Meteor Comm Corp
    ATTN: R. Leader

Mission Research Corp
    ATTN: C. Lauer
    ATTN: F. Fajen
    ATTN: F. Guigliano
    ATTN: G. McCartor
    ATTN: R. Bigoni
    ATTN: R. Bogusch
    ATTN: R. Dana
    ATTN: R. Hendrick
    ATTN: R. Kilb
    ATTN: S. Gutsche
    ATTN: Tech Library
2 cys ATTN: D. Knepp
5 cys ATTN: Doc Control

Mitre Corp
    ATTN: J. Wheeler
    ATTN: M. Horrocks
    ATTN: W. Foster
    ATTN: W. Hall

Pacific-Sierra Research Corp
    ATTN: E. Field, Jr
    ATTN: F. Thomas
    ATTN: H. Brode, Chairman SAGE

Pennsylvania State University
    ATTN: Ionospheric Rsch Lab

Photometrics, Inc
    ATTN: I. Kofsky

Physical Dynamics, Inc
    ATTN: E. Fremouw
    ATTN: J. Secan

Physical Rsch, Inc
    ATTN: K. Schueter
    ATTN: R. Deliberis
    ATTN: T. Stephens

Physical Research, Inc
    ATTN: J. DeVore
    ATTN: J. Thompson

R&D Associates
    ATTN: B. Yoon

R&D Associates
    ATTN: G. Ganong

R&D Associates
    ATTN: C. Greifinger
    ATTN: F. Gilmore
    ATTN: G. Stcyr
    ATTN: H. Ory
    ATTN: M. Gantsweg
    ATTN: R. Turco
    ATTN: W. Karzas
    ATTN: W. Wright
    ATTN: P. Haas

Rand Corp
    ATTN: C. Crain
    ATTN: E. Bedrozian
    ATTN: P. Davis

Rand Corp
    ATTN: B. Bennett

Riverside Rsch Institute
    ATTN: V. Trapani

Rockwell International Corp
    ATTN: R. Buckner

Rockwell International Corp
    ATTN: S. Quilici

Science Applications Intl Corp
    ATTN: E. Szuzewice
    ATTN: J. Cockayne

Science Applications, Inc
    ATTN: R. Heimiller

Science Applications, Inc
    ATTN: C. Smith
    ATTN: D. Hamlin
    ATTN: D. Sachs
    ATTN: E. Straker
    ATTN: L. Linson

Science Applications, Inc
    ATTN: M. Cross

Signatron, Inc
    ATTN: S. Pair

SRI International
    ATTN: A. Burns
    ATTN: C. Rino
    ATTN: D. McDaniels
    ATTN: D. Neilson
    ATTN: G. Price
    ATTN: G. Smith
    ATTN: J. Petrickes
    ATTN: J. Vickrey
    ATTN: M. Baron
    ATTN: R. Leadabrand
    ATTN: R. Livingston
    ATTN: R. Tsunoda
    ATTN: V. Gonzales
    ATTN: W. Chestnut
    ATTN: W. Jaye

Stewart Radiance Laboratory
    ATTN: R. Huppi

DEPARTMENT OF DEFENSE CONTRACTORS (Continued)

Swerling, Manasse & Smith, Inc
    ATTN: R. Manasse

Syracuse Rsch Corp
    ATTN: R. Herman

Technology International Corp
    ATTN: W. Boquist

Toyon Rsch Corp
    ATTN: J. Garbarino
    ATTN: J. Ise

TRA Electronics & Defense Sector
    ATTN: R. Plebuch

Mitre Corp
    ATTN: A. Kymmel
    ATTN: C. Callahan
    ATTN: G. Harding
    ATTN: MS J104, M. Dresp

DEPARTMENT OF DEFENSE CONTRACTORS (Continued)

Utah State University
Attention Sec Control for
    ATTN: K. Baker
    ATTN: A. Steed
    ATTN: D. Burt
    ATTN: L. Jensen

VisiDyne, Inc
    ATTN: C. Humphrey
    ATTN: H. Smith
    ATTN: J. Carpenter
    ATTN: O. Shepard
    ATTN: W. Reidy

END

FILMED

8-85

DTIC